

MULTIOMICS AND DIGITAL MONITORING DURING LIFESTYLE CHANGES REVEAL INDEPENDENT DIMENSIONS OF HUMAN BIOLOGY AND HEALTH

Francesco Marabita^{1,2}, Tojo James^{1,2}, Anu Karhu¹, Robert Mills¹, Teemu Perheentupa¹, Hans Stenlund³,
Fredrik Boulund⁴, Cecilia Hellström⁵, Maja Neiman⁵, Heidi Virtanen¹, Kaisa Kettunen^{6,1}, Hannele
Laivuori^{1,7,8}, Pyry Helkkula¹, Myles Byrne¹, Harri Honko⁹, Antti Kallonen⁹, Miikka Ermes¹⁰, Heidi Similä¹⁰,
Mikko Lindholm¹⁰, Elisabeth Widen¹, Samuli Ripatti¹, Maritta Perälä-Heape^{11,12}, Lars Engstrand⁴, Peter
Nilsson⁵, Thomas Moritz^{3,13}, Timo Miettinen¹, Riitta Sallinen^{1,2}, Olli Kallioniemi^{1,2}

¹Institute for Molecular Medicine Finland (FIMM), HiLIFE, University of Helsinki, Helsinki, Finland. ²Science for Life Laboratory, Department of Oncology-Pathology, Karolinska Institutet, Stockholm, Sweden. ³Science for Life Laboratory, Swedish Metabolomics Centre, Department of Forest Genetics and Plant Physiology, Swedish University of Agricultural Sciences, Umeå, Sweden. ⁴Science for Life Laboratory, Center for Translational Microbiome Research, Department of Microbiology, Tumor and Cell biology, Karolinska Institutet, Stockholm, Sweden. ⁵Science for Life Laboratory, Division of Affinity Proteomics, Department of Protein Science, KTH Royal Institute of Technology, Stockholm, Sweden. ⁶HUS Diagnostic Center, Laboratory of Genetics, University of Helsinki and Helsinki University Hospital, Helsinki, Finland. ⁷Medical and Clinical Genetics, University of Helsinki and Helsinki University Hospital, Helsinki, Finland. ⁸Department of Obstetrics and Gynecology, Tampere University Hospital and Tampere University, Faculty of Medicine and Health Technology, Tampere, Finland. ⁹Tampere University of Technology, Tampere, Finland. ¹⁰VTT Technical Research Centre of Finland, Espoo, Finland. ¹¹Faculty of Medicine, University of Oulu, Oulu, Finland. ¹²Centre for Health and Technology, University of Oulu, Oulu, Finland. ¹³Novo Nordisk Foundation Center for Basic Metabolic Research, Faculty of Health and Medical Sciences, University of Copenhagen, Copenhagen, Denmark.

ABSTRACT

We collected clinical measurements, health surveys and multiomics profiles (genomics, proteomics, autoantibodies, metabolomics and gut microbiome) from 96 individuals over 16 months, along with daily activity and sleep monitoring. Between- and within-individual variability was analysed as the participants underwent data-driven health coaching. Multiomics factor analysis resulted in an unsupervised integrated view of the data, with individual factors explaining distinct aspects of variability in human health and lifestyle, such as obesity, diabetes, liver function, cardiovascular disease, inflammation, immunity, hormonal function, exercise and diet. The data revealed both known and new associations between molecular pathways, risk factors, behaviour and lifestyle aspects. Data-driven analysis of multidimensional molecular and digital signatures of participants over time enabled deep understanding of biological variability between people as well as the systemic effects of lifestyle changes. Our study facilitates a detailed evaluation of aspects impacting on health and underlines the importance of personal molecular signatures.

40 Monitoring of human health, impact of lifestyle and disease development is possible by
longitudinal measurements of clinical laboratory tests, omics technologies, or digital health monitoring
42 using wearable sensors. This provides opportunities to explore human systems biology and to predict
and intervene in processes leading to disease development. However, our knowledge and ability to
44 make use of such data and define actionable insights, correlations and causal patterns are limited.
There is a lack of deep integrated datasets, where different dimensions of human biology have been
46 explored at the same time. Each individual has a unique profile, composed of genetic, epigenetic,
molecular, clinical and lifestyle parameters, which may change over time during development, aging
48 and disease transitions. These processes cannot be understood as a single general pathway for the
average human or patient, but they can best be described as a collection of individual trajectories.
50 Several studies have investigated the use of individualized molecular profiles to assess disease risks
or the connection between omics measurements and clinical tests, using an n-of-one longitudinal
52 approach^{1,2}, a cross-sectional design³, a controlled longitudinal perturbation study⁴, or a cohort study
with personal behavioural coaching⁵. More recently, other studies⁶⁻⁸ analysed longitudinal data over
54 an extended time period in a cohort of individuals at risk for diabetes, while another prospective
observational study investigated the stability of the individual molecular signatures⁹.

56 The Digital Health Revolution (DHR) program¹⁰ in 2015-2020 was based on the concept that future
healthcare strategies will evolve in a direction which allows citizens to control and make use of their
58 own personal data to improve their health and wellness. The project aimed at implementing proactive
P4 (predictive, preventive, personalized, and participatory) healthcare with multi-level molecular and
60 digital data. Within this framework, we integrated deep multi-omics profiles and connected them to
health surveys, clinical observations and digital health measurements. We aimed to: 1) integrate
62 longitudinal multi-omics data between and within people over time; 2) exploit the discovered
associations to understand novel links between molecular and clinical data; and 3) verify if data
64 feedback and coaching would guide and motivate people to make lifestyle changes. Overall, we aimed
at achieving a holistic understanding of the variables involved in different aspects of human biology
66 and health. To accomplish these goals, we applied multi-omics factor analysis and connected the
learned factors with interpretable features of health and behaviour.

68 RESULTS

STUDY OVERVIEW

70 We carried out a 16-month longitudinal study on 96 individuals (aged 25-59) recruited from an
occupational healthcare clinic in Helsinki, Finland (Supplementary Figure 1-2 and Supplementary Table
72 1). The participants had no previously diagnosed serious chronic diseases, although we allowed
individuals with risk factors for chronic diseases. We acquired comprehensive measurements of health
74 and behaviour, including anthropometrics, clinical laboratory tests, questionnaire data, physical fitness
tests and activity and sleep quantification with a wearable device. In addition, we performed a series
76 of omics measurements to study the genome, the plasma proteome and metabolome, the
autoantibody profile and the gut microbiome. The prospective collection of molecular and digital
78 profiles resulted in a thorough longitudinal dataset of human health and lifestyle aspects (Figure 1).
This allowed to define baseline molecular profiles and longitudinal trajectories of health data in the
80 participants during a personalized lifestyle coaching. We collected over 20,000 biological samples
during five study visits and generated a compendium of >53 million primary data points, for 558,032
82 distinct features. Two types of feedback were applied to stimulate and motivate lifestyle changes.
First, actionable health data were returned to participants through a web dashboard and interpreted
84 by a study physician, starting from the second visit. Second, personal data-driven coaching was
provided, including three face-to-face and six remote meetings, plus continuous email and phone
86 support, starting from the third visit. Personal actionable possibilities were identified with the help of
questionnaires, clinical laboratory tests and physical examination, and focused on diet, exercise,
88 mental wellbeing, stress and time management. Of the 107 people enrolled, 96 completed the study.
The data-driven coaching positively impacted on the health of the participants, and 86% reported
90 subjective improvement in at least of the following aspects: diet, exercise, sleep, mental wellbeing,
stress management, drinking or smoking (Supplementary Figure 3). For example, the percentage of
92 people who did not exercise decreased from 9% to 1%, the percentage of smokers decreased from
16% to 8%, and the percentage of daily drinkers from 8% to 5%. The participants felt that the wearable
94 device, return of personal health data, and tailored coaching were the most motivating aspects of the

study. Overall, the subjects were enthusiastic about participating and 76% indicated that they would
96 again take part in a similar study.

LONGITUDINAL ACTIONABLE CHANGES

98 We defined a *phenotype* using the ensemble of questionnaires, anthropometrics, vitals and clinical
laboratory tests. Actionable health issues were defined at baseline, including dyslipidaemia,
100 overweight and obesity, elevated systolic blood pressure, low vitamin D, elevated blood glucose,
anaemia and self-reported obstructive sleep apnea (Supplementary table 1 and Supplementary Figure
102 4).

We first analysed the clinical measurements at baseline to define the group of individuals with Out-Of-
104 Range (OORB) values. To explore if the data feedback and coaching had a positive effect on objective
health parameters, we modelled the longitudinal changes in the OORB individuals, based on the
106 assumption that measurements outside the reference values represented an actionable finding to
improve lifestyle and health. We analysed the average change per visit, adjusting for sex and age. We
108 found significant improvements ($FDR < 0.05$) in several key health parameters for the OORB group
during the course of the study, such as an increase in vitamin D levels and a decrease in blood
110 pressure, LDL-cholesterol, and total/HDL cholesterol ratio (Figure 2 and Supplementary Table 3).

Secondly, we obtained an overview of all the clinical variables and compared the individuals using
112 Principal Component Analysis (PCA). The first three PCs (Figure 2) accounted for 44.8% of the variance
and the major drivers of variability were cardiometabolic variables (for PC1 and PC3: BMI, insulin,
114 fasting glucose, cholesterol, and lipoprotein profiles) and sex-dependent anthropometrics and
hematological measurements (PC2). Trajectories for selected individuals showed the changes during
116 the multiple study visits and visualized the improvements in the clinical parameters (Figure 2 and
Supplementary Figure 5).

118 In summary, we showed that the return of data as well as data-driven lifestyle coaching resulted in
objective improvements of health behaviour and health outcomes, including physiological and
120 laboratory measurements indicative of cardiovascular risk.

MULTIOMICS SIGNATURES

122 *DISTINCT SOURCES OF MOLECULAR VARIABILITY*

We next generated multiomics profiles and set out to explore the association of these variables with
124 each other and with the clinical features. We first investigated the sources of variability in the omics,
by partitioning the variance for each feature into personal variation (i.e. between-individual), known
126 factors (age, sex and study visit) and residual unknown sources (for example biological, environmental
or technical aspects). We found that the personal variation impacted all data types but to a different
128 extent (Supplementary Figure 6). Autoantibodies represented a highly personal signature and on
average 92% of the variance was explained by personal variation. Metabolites were dominated by
130 personal variation (56-71% on average) but residual components were also present (23-35% on
average). Proteins had similar average personal (49%) and residual components (45%). The
132 microbiome data was dominated by unexplained factors (68% on average). These results were
confirmed by an alternative distance-based method (Supplementary Figure 6). We observed that the
134 average within-individual distance was lower than the between-individual distance, to a different extent
for different omics, and autoantibodies showed the lowest within-individual distance, i.e. high
136 similarity.

UNDERSTANDING THE MOLECULAR VARIABILITY

138 We used Multi-Omics Factor Analysis (MOFA+)^{11,12} to carry out an unsupervised analysis of the
complete multiomics data, hence excluding the clinical variables and other phenotypic data. MOFA+
140 helped to integrate and interpret the measurements and their variability across all the omics layers.
MOFA+ resulted in an interpretable low-dimensional representation in the form of a small number of
142 independent factors that captured the major sources variability in the data and originated from
simultaneous inclusion of baseline and longitudinal differences. The analysis facilitated the
144 identification of subgroups of samples and the molecular features that contributed to the ordination of

the samples in the dimensions defined by the factors. An overview of the samples based on the learned
146 factors is given in Supplementary Figure 7. We identified 14 factors (F1-F14), each explaining a
minimum of 2% of the variance in at least one data type. The fraction of the total variance explained
148 across the six omics types varied from 6% for gut microbiome to 95% for the autoantibodies (Figure
3). The learned factors were either predominantly associated with one omics type or contributed to
150 several omics types, suggesting that the underlying biological determinants might affect different types
of measurements simultaneously. We then explored the molecular basis of each factor. First, we
152 investigated the contribution of the original omics features, by inspecting the loadings on each factor,
which represent their weights, in order to interpret the nature of the associated biological domains.
154 Second, we tested the association between the factors and the phenotype, including questionnaire
data, clinical variables, fitness tests, activity and sleep data, and other metrics. Each factor was linked
156 to specific phenotypic characteristics (linear models, $FDR < 0.001$, Figure 3 and Supplementary Table
4). Importantly, most of the factors were associated with distinct sets of variables across the different
158 categories and thereby defined molecular patterns that were linked to distinct aspects of lifestyle and
health, including modifiable behavioural aspects, such as diet and exercise. We then refined the top
160 associations for each factor with a covariate-adjusted statistical model. We aimed at accounting for
the correlation among observations from the same individual and fitted a linear mixed model (LMM),
162 with age and sex as fixed effects and the individual as a random effect. We also interpreted the
association in view of the contributing molecular features and pathways and the results are presented
164 below.

Obesity and insulin resistance. The top features with high positive loadings on F11 included plasma
166 proteins involved in pathways known to be dysregulated in obesity or dyslipidemia (LEP¹³, IL-1ra
(IL1RN)¹⁴, t-PA (PLAT)¹⁵, FABP4¹⁶, FGF21¹⁷, IL-6¹⁴, LDL receptor¹⁸). Interestingly, several proteins
168 reported as protective factors against obesity (GH1, IGFBP1, PON3)¹⁹⁻²¹ had negative loadings. We
found significant correlations between F11 and well-known metabolic traits and clinical measurements
170 (Figure 4 and Supplementary figure 9). These included positive association with BMI ($p_{lmm}=1.53E-21$),
LDL-cholesterol levels ($p_{lmm}=4.47E-03$) and insulin resistance ($\log_{10}HOMA-IR$, $p_{lmm}=6.51E-14$). Also,

172 we found a negative association with HDL-cholesterol ($p_{imm} = 2.16E-06$) as well as with measures of
physical activity and fitness gathered from the questionnaire, such as leisure-time exercise
174 ($p_{imm}=1.06E-03$) and exercise habits ($p_{imm}=8.25E-04$), or the activity levels in terms of steps/day
measured by the wearable device ($p_{imm}=0.01$). An inverse correlation was also observed with physical
176 fitness at the level of upper body ($p_{imm}=5.53E-05$) abdominal ($p_{imm}=1.59E-03$) and lower body
($p_{imm}=1.14E-03$). Participants with first-degree relatives with diabetes had higher factor values
178 compared to the individuals who did not report family-history for diabetes ($p_{imm}=6.25E-03$). Finally, an
individual who was diagnosed with type 2 diabetes during the study had the highest factor values. We
180 therefore interpreted F11 as strongly related to obesity, insulin resistance and diabetes risk and
pathogenesis as well as clearly associated with quantitative data on exercise and mobility. F11 was
182 also associated with overall health, as evidenced by a negative association with self-reported overall
health ($p_{imm}=9.26E-07$) and a positive correlation with predicted coronary heart disease (CHD) risk
184 ($p_{imm}=0.01$). In summary, F11 assisted in estimating molecular patterns of health and behaviour that
are associated with obesity as well as potential trajectories leading to diabetes.

186 **Impact of hormones and ethinyl estradiol.** F9 was influenced by sex and sex-specific biological
differences in multiomics. In contrast, F14 was linked to the use hormone replacement therapy or
188 hormonal contraception in women. Particularly, young women reporting the use of a contraceptive
containing ethinyl estradiol (EE) had elevated F14 values ($p_{imm}=2.28e-10$). F14 appeared to be almost
190 exclusively linked to the use of EE. Consistent with this observation, known estrogen-sensitive proteins
had the highest positive weights for F14 (Figure 4), but there were also contributions from cortisol and
192 thyroxine levels, which we interpreted as potential secondary effects^{22,23}. Pulse ($p_{imm}=9.32E-03$),
hsCRP (log-transformed, $p_{imm}=7.40E-09$) and leukocyte numbers (log-transformed, $p_{imm}=6.09e-05$)
194 also positively correlated with F14 and alterations of these clinical laboratory parameters were
prominent in women with particularly high factor values. These observations indicated that EE use is
196 associated with strong and distinct effects on human biology, which may lead to increased levels of
inflammation, impact on thyroid and cortisol levels as well as physiological effects.

198 **Dietary habits.** F3 and F6 were mostly connected to the metabolome, they were associated with
dietary habits (Supplementary figure 10), such as reported consumption of fresh fruit and vegetables.
200 However, all the predictors were not significantly associated to the factors ($p_{\text{imm}} > 0.05$) in the covariate-
adjusted models, suggesting that the association may be explained by individual-specific (person-to-
202 person) differences and not by changes of the diet during the study. Moreover, caffeine and its
metabolites were abundantly represented among the features with largest loadings for F7 (Figure 4),
204 and indeed this factor was strongly correlated with self-reported coffee consumption ($p_{\text{imm}} = 7.63E-12$).

Lipids, free fatty acids and fatty acid esters. F5, F8 and F12 (Supplementary figure 11) were each
206 associated with distinct aspects of plasma lipid composition. In particular, free fatty acids (FFA)
contributed mostly to F12, while fatty acid esters (FAEs), mostly in the form of acylcarnitines,
208 contributed to F5 and F8. In the postabsorptive state, blood FFA are a result of lipolysis from adipose
tissue and they reflect dietary intake²⁴, while changes in the acylcarnitine pool can be linked to changes
210 in fatty acid oxidation. Accumulation of acylcarnitines as products of incomplete mitochondrial fatty
acid oxidation has been associated with obesity and diabetes²⁵. Even after adjusting for the covariates,
212 F12 was negatively associated with blood pressure (systolic, $p = 0.035$; diastolic $p = 0.021$), in line with
the known association between FFA and hypertension²⁶. F5 and F8 were both strongly associated with
214 clinical measurements indicating dyslipidemia, including total cholesterol ($p_{\text{imm}} = 1.64E-08$ and
 $p_{\text{imm}} = 8.48E-10$) LDL cholesterol ($p_{\text{imm}} = 7.13E-06$ and $p_{\text{imm}} = 1.74E-05$), triglycerides ($p_{\text{imm}} = 3.74E-05$ and
216 $p_{\text{imm}} = 8.45E-7$) and ApoB ($p_{\text{imm}} = 3.24E-08$ and $p_{\text{imm}} = 9.11E-06$), thus implicating dysregulation of lipid
metabolism as an underlying influence for F5 and F8. Importantly, they were only weakly associated
218 with BMI ($R^2 = 0.004$ and $R^2 = 0.006$; $p_{\text{imm}} = 0.05$ and $p_{\text{imm}} = 0.07$), suggesting that these two factors were
associated with dyslipidemia independently of obesity. Sex was a significant covariate for the
220 associations seen for F5 (maximum $p_{\text{imm}} = 1.21E-05$) but not for F8 (minimum $p_{\text{imm}} = 0.73$).

Hepatic function. Metabolites connected to liver function had major loadings on F2 (Supplementary
222 figure 12). Bile acids or their glycine or taurine conjugates had negative weights and a major impact in
the classification of the individuals along the F2 axis. The involvement of the liver function in
224 determining F2 values was supported by the contribution of other liver-associated metabolites that on

average were increased in the samples with negative factor values. These metabolites are known to
226 be increased in blood after liver disease (biliverdin) or used to eliminate the hepatic nitrogen pool
(glutamine, hippuric acid, phenylacetylglutamine). The liver is a fundamental organ in maintaining
228 metabolic homeostasis, it modulates the composition of the blood metabolome and therefore we
assumed that F2 reflected the structural and functional integrity of the liver.

230 **Autoantibodies.** F1 was mostly explained by the presence of autoantibodies, which did not contribute
importantly to other factors. F1 was influenced by the binary nature of the autoantibody data
232 (presence/absence) and due to the stable autoantibody signature over time. Indeed, autoantibodies
can be considered as an IgG reactivity barcode for each individual²⁷. F1 correlated well with the
234 autoantibody counts and to a lesser extent with the age (Supplementary Figure 8), in agreement with
the fact that autoreactivity is more common in the elderly, possibly linked to age-associated B cells²⁸.

236 In summary, we demonstrated that we could understand the pattern of molecular variation by
exploiting the factors, each reflecting distinct types of human biology, behaviour, lifestyle, hormonal
238 use or potential transitions to disease.

CORRELATION NETWORK

240 We performed a correlation analysis, including all the multiomics data as well as an ensemble of
quantitative or semi-quantitative measures consisting of clinical data, activity and sleep, fitness test
242 data, and other scores. We computed a cross-correlation network between features of different types
using two alternative metrics. For the between-individuals network (BIN), we averaged the
244 measurements from all time points before calculating correlations between features. We also included
146 genetic trait scores obtained by summing up the contribution from all the variants associated with
246 each trait as reported by the GWAS catalog. The within-individuals network (WIN) consisted of linear
correlations of repeated measures of pairs of features within-participants. It estimated a common
248 regression slope, representing a measure of association shared among individuals, and resulting from
changes occurring at the individual level during the study. The BIN and WIN were calculated after age-

250 and sex-adjustment and p-values were corrected for multiple hypothesis (FDR<0.05). We then
identified distinct communities of interconnected features (modules), as an aid for interpretation.

252 Among the strongest correlations of the BIN ($|\rho| > 0.6$), we detected not only pairs measuring the same
molecular entity using different assays (i.e. TSH (clinical-PEA), $\rho= 0.96$; Cholesterol (clinical-GCMS)
254 $\rho=0.82$), but also features of different types, for example LDL-receptor protein and triglycerides
($\rho=0.82$) or LEP protein and BMI ($\rho=0.68$). The network consisted of 375 nodes and 570 edges
256 (Supplementary table 5). Several clinical variables represented hubs with the largest number of
associated connections to metabolites and proteins (Figure 5). Those hubs were inversely correlated
258 to modifiable behavioural risk factors, consisting in wearable-based measures of physical activity
(intense physical activities to insulin, number of steps to waist circumference). Similarly, measures of
260 physical fitness (lower body, abdominal and upper body) inversely correlated with LEP. Notably, the
proteins with common genetic defects in familial hypercholesterolemia figured in the cardiometabolic
262 subnetwork, namely LDLR, PCSK9, and apolipoprotein. For instance, PCSK9, a pharmacological
target of LDL-lowering therapies, correlated positively to several glycerophospholipids and ApoB, but
264 negatively to CMPF (3-Carboxy-4-methyl-5-propyl-2-furanpropionic acid), a metabolite that is formed
from the consumption of fish oil and may have positive metabolic effects²⁹. In the whole network, 24
266 GWAS summary scores resulted significantly associated with at least one other node (Supplementary
figure 13), and 11 scores concerned haematological measurements (erythrocytes, leucocytes and
268 thrombocytes). While some edges associated the genetic score directly with the corresponding trait
measured in this study, especially for haematological traits, other associations occurred between
270 proteins or metabolites and the genetic susceptibility to a disease/trait with cardiometabolic relevance.
For example, we observed an inverse association between the score for BMI in physically inactive
272 individuals and several FAEs, carnitine and tyrosine. Furthermore, an inverse association was observed
between the score for abdominal aortic aneurysm and IL-6RA levels, supporting the contribution of IL-
274 6 signalling and inflammation to this disease³⁰. These observations indicated that the between-
individuals variability might be explained at least partly by personal genetic differences.

276 The WIN captured associations between pairs of features that resulted from concordant variation in
repeated measures obtained from the same individuals. This source of variation is assumed to be
278 complementary to the BIN, it does not average or aggregate the data, neither does it violate the
assumption of independence of the observations. We interpreted the edges in this network as
280 associations resulting from changes occurring over time and not due to baseline between-individuals
characteristics. The network consisted of 302 nodes and 611 edges (Supplementary table 5). Only 46
282 edges and 151 nodes were also detected in the BIN, suggesting that a non-overlapping set of
correlations were represented. For example, in an inflammation-related subnetwork (Figure 5), hsCRP
284 and leucocytes lay in the proximity of cytokines, cytokine receptors, proteins involved in leukocyte
functions and members of the tryptophan metabolic pathway (kyneurine and indoles). This subnetwork
286 was not revealed in the BIN and the observed edges likely originate from individuals transitioning
through inflammatory states or infections during the study, although we cannot completely exclude
288 seasonal variation. Other edges specifically observed in the WIN positioned measures of activities and
sleep in the proximity of several metabolites and proteins. Among the proteins, we observed well-
290 known members of lipid metabolism pathways (LEP, LPL) and proteins with related functions
(PTX3^{31,32}, NRP1³³, PRSS8³⁴). Correspondingly, FFA and FAEs appeared in this subnetwork. The above
292 correlations suggested that within-individual dietary factors, changes in fat metabolism and changes
in physical activity could be further investigated as motivations for the observed associations.
294 Furthermore, the connection with sleep and physical activity is reminiscent of the link between leptin,
circadian rhythm, sleep quality, and obesity³⁵.

296 PERSONAL TRAJECTORIES

In order to stimulate lifestyle changes and improve health, we defined personalized, actionable
298 possibilities for each participant. This strategy resulted in groupwise significant changes in actionable
clinical variables. When considered individual-wise, the changes unfolded into personal trajectories,
300 and often a connection with the multiomics was established. Common behavioural adjustments were
related to diet and exercise, illustrated by the case of a 28-year male. The subject underwent positive
302 adaptations resulting in improvement of clinical variables and self-rated health (Figure 2 and Figure 6),
in agreement with the nutritional and exercise recommendations. At baseline, he presented with

304 obesity, high systolic blood pressure, dyslipidaemia, elevated insulin levels and elevated hsCRP
(Figure 6A). During the study, he reported increases in self-rated health, frequency and amount of
306 exercise (Figure 6C), and these adaptations were confirmed by the activity levels detected by the
wearable device (Figure 6B). The sustained level of activity resulted in longitudinal changes in key
308 actionable clinical variables at the end of the study (Figure 6A), including decreased BMI, improved
lipid profile, reduced low-grade systemic inflammation, reduced systolic blood pressure, normalization
310 of insulin levels and improvement of the estimated insulin resistance. These interpretable changes
reflected variation in the omics domain as well, as shown by the MOFA+ factors (Figure 6D). Indeed,
312 the improvement in the BMI, lipid profile and insulin resistance, combined with an increase in physical
activity, is compatible with the observed decrease in F11 values for this subject. We indeed observed
314 longitudinal decrease of obesity- and inflammation-associated proteins and other adaptations
suggesting an involvement of the GH/IGF-1 axis. Similarly, the changes in F8 and F10 - associated
316 with fatty acid esters and lipid metabolism - reflected the variation in the total cholesterol levels.
Several acylcarnitines peaked at the third visit, suggesting a metabolic adjustment during a transition
318 period toward increased physical activity. For comparison, we show (Figure 2 and Supplementary
figure 14) the case of a 36-years female, presenting obesity, dyslipidaemia, hyperinsulinemia and
320 hyperglycaemia at baseline. She was referred to consult her physician and was indeed diagnosed with
type 2 diabetes. During the study, phenotypic changes occurred: reduction in the glucose, insulin and
322 cholesterol levels, as a result of therapeutic intervention (Metformin, Atorvastatin, Empagliflozin) and
not a genuine lifestyle change with increased physical activity. Correspondingly, the levels of the
324 MOFA+ factors did not change considerably and this individual remained an outlier at all the time
points.

326 The case of participant with a respiratory tract infection is illustrated in Supplementary Figure 15, it
shows the dysregulation of metabolic pathways during infection as previously observed^{1,6}, and it
328 highlights the importance of personal metabolic signatures which can be altered during infections.

330 DISCUSSION

The convergence of systems medicine, digital health, big data, consumer-driven healthcare and social
332 networks is at the heart of the P4 healthcare model. To promote the P4 approach into the current
healthcare systems, longitudinal personalized health intervention studies are needed, and numerous
334 initiatives exist to profile healthy individuals according to the precision medicine principle. However,
fewer studies have simultaneously combined longitudinal multiomics profiling, digital self-tracking and
336 health monitoring, data feedback and tailored lifestyle coaching. We have done all this with a
comprehensive approach and generated a valuable longitudinal data set which can serve both as a
338 resource and a reference for future precision medicine studies. Our study has provided several steps
in the context of precision medicine. Firstly, by adding layers of molecular information and long-term
340 monitoring on top of genomics, we have stressed the importance of including multiomics profiling
other than genomics to precision medicine initiatives. Indeed, current large-scale academic and
342 commercial initiatives largely rely on genetic data connected to health outcomes, while there is a need
for expanding the precision medicine toolbox to include multiomics and functional assays, especially
344 in precision oncology^{35,36}. Secondly, by integrating the molecular data with digital health parameters,
we have demonstrated that a connection between the molecular environment and the external
346 manifest characteristics (*phenotype*) occurs and concerns a multiplicity of health and lifestyle aspects,
collected with traditional and emerging modalities, and including adiposity, hormonal influences, diet
348 and physical activity, to mention a few. Our holistic efforts resulted in an unsupervised re-discovery of
known associations between molecular features and indicate that changes in measures from a
350 consumer health wearable device are connected with changes in molecular features. Thirdly, our study
design implemented data feedback and coaching to stimulate lifestyle changes and we anticipate that
352 this model could become broadly applicable to future efforts. However, only information derived from
the genetic data was actively returned to the participants, while the other multiomics data were
354 generated at the end of the study, mostly to minimize systematic biases and batch effects. Currently,
this challenge remains to be solved, especially in the context of precision medicine, where collections
356 can be assembled from n-of-one experiments and longitudinally collected samples, but systematic
biases are common due for example to systematic variations of instrument responses or reagents lots.

358 Our analysis proposed a low-dimensional space to investigate the complexity of the multiomics and
the connection to known sources of variation. Among those, sex, age and BMI are among the most
360 studied and often are confounders in association models. For this reason, we regressed out the effect
of age and sex in the correlation networks, but we allowed the effect of these covariates to appear in
362 the MOFA+ analysis, in order to verify if separate axes of variability could be retrieved and if they were
independent of them. Indeed, we verified that BMI, as a proxy for adiposity and obesity, could only be
364 strongly associated with one factor but it did not influence relevantly the others. Similarly, age and sex
associated to a few but not all factors, showing that the identified axes of variation represented a
366 spectrum of molecular variation connected to several lifestyle factors, which cannot simply be
explained by the most common predictors mentioned above.

368 One interesting observation is that the use of oral contraceptives containing EE is alone a sufficient
element to influence the covariance of the proteome and metabolome, to such extent that one of the
370 identified factors is nearly an indication of the use of this drug. These effects were identified in a data-
driven manner and we discovered a distinct dimension of variability in human biology influenced by an
372 external hormone, whose effects are strong enough to be clearly picked up in an unsupervised
analysis, above all other causes of variability and noise. F14 could therefore be a potentially useful
374 metric to assess exposure to EE as well as associated health effects. Besides being the major female
hormone, estrogen is a fundamental hormone for the maintenance of tissue homeostasis of several
376 tissue types in both males and females, and therefore it is not unexpected that modulation of this
pathway has detectable consequences in the proteome and metabolome. However, considering that
378 the exposure to EE from contraceptives could be long-term, what remains to be investigated is either
the biological significance of this persistent alteration, but also to what extent this covariate is generally
380 unaccounted in multiomics screens, in view of the fact that similar alterations could be associated to
other physiopathological conditions. For example, serum TFF3 was found to be elevated in women
382 with breast cancer³⁶, and FETUB is a highly abundant liver-secreted protein sensitive to estrogen and
increased in type 2 diabetes^{37,38}.

384 Our analysis showed that part of the variability in the multiomics features could be explained by genetic
determinants. This raised the question whether an interaction could exist between the genetic
386 predisposition and the magnitude of the changes observed in clinical and omics variables. We have
addressed this subject specifically for the levels of 25(OH)D (vitamin D) and tailored the
388 supplementation guided by genetic markers. The results are presented elsewhere (Sallinen et al., The
Journal of Nutrition, in press) and support the evidence that genetic predispositions impact the
390 response to certain lifestyle changes and interventions^{39,40}.

While the average individual does not exist, empirical evidence and conclusions based on large groups
392 of individuals and summary measures are the norm in experimental research. Under the paradigm of
precision medicine and health, this assumption is mitigated by the application of treatment and
394 prevention strategies taking into account the individual variability. However, when highly dense
longitudinal multiomics and phenotyping studies are performed, the challenges and drawbacks of
396 aggregating personal profiles are increasing. For example, the presence of outlier measurements for
some individuals could be explained by the occurrence of specific events detected by traditional
398 methods or inferred from the use of wearable devices. Indeed, the use of wearable devices offer the
opportunity of continuously monitoring the participants, therefore allowing the detection of acute
400 events or behaviours that would be missing when registering outcomes with traditional methods or
when averaging across time. Our data contribute to the accumulating evidence that personal
402 multiomics signatures show individual dynamics and associate with specific physiological or
pathological events^{1,6,7}.

404 We have to acknowledge limitations of our study. Firstly, the small sample size limits the discovery of
novel associations and implies that the conclusion should be confirmed in larger cohorts to have
406 further empirical evidence. Nevertheless, we retrieved several known associations, likely resulting from
strong underlying effect sizes. For example, we showed that several blood cell measures in our study
408 are under genetic control, in agreement with the high heritability of hematological traits⁴¹. By extension,
it is possible that the associations with cardiometabolic relevance observed in our study have also
410 larger true effect sizes. While this is a limitation for the discovery of unknown relationships, it is on the

contrary important from the translational point of view, because our study qualifies as a resource for
412 extracting further candidate investigations, especially in medically relevant terms.

Because of the highly personalized, non-structured nature of the coaching, our work does not strictly
414 qualify as an interventional study, and we have to recognize the lack of a proper control group not
receiving data feedback and coaching. A certain heterogeneity in the individual adherence to the
416 recommendations might bias the conclusions based on aggregated measures. We have shown that
individual trajectories and multiomics profiles exists and our data collection can propose certain
418 connections only when specific cases were considered. For example, in the case of activity and sleep
tracking, we observed good overall engagement, although the compliance over time was not constant
420 for all the individuals. In addition, a certain seasonality cannot be excluded and indeed periodicity in
immune systems gene expression and cellular composition is often investigated^{42,43}. Therefore,
422 seasonality might have a contribution in influencing the changes occurring at the within-individual level.

Our study is truly a forerunner in shaping person centric data driven care for the future. It demonstrated
424 not only the power of combination of multi-omics data and lifestyle data, but new opportunities for the
healthcare system to design their services towards predictive data-driven care and support individuals
426 in lifestyle changes. New data sets, like multiomics measurements and continuous monitoring via
wearable devices will shape the traditional disease-based healthcare. However, more research is
428 needed to truly enhance the proactive, personalized health maintenance for the benefit of individuals,
and society.

430

METHODS

432 *ETHICAL PERMIT AND CONSENT*

The study was conducted in line with the Declaration of Helsinki and approved by the Coordinating
434 Ethics Committee of the Helsinki University Hospital, Finland. Each participant provided informed
written consent for the study and the biobanking of samples and data. Participants were free to drop
436 out any time, but their samples and data were still available for analyses. If a participant withdrew the
consent, samples and data were discarded.

438 *OVERVIEW*

The study was conducted at the Institute for Molecular Medicine Finland (FIMM), HiLIFE, University of
440 Helsinki, Finland, between September 2015 and January 2017. Recruitment was performed in
September 2015, and five study visits followed, approximately every four months, (Supplementary
442 Figure 1). Every visit included a health check-up and blood and urine sampling. Before or after every
visit, participants collected fecal and saliva samples, filled out a questionnaire, and performed fitness
444 tests. Data on physical activity and sleep was collected from the second visit onward with an activity
watch. Key actionable health data were returned to the participants via a web dashboard starting at
446 the second visit. Tailored health and wellness advice and coaching was provided by two personal
trainers from the third visit onward. Between visits 4 and 5, participants could compare their data to
448 summary measures calculated with the other participants' data.

ELIGIBILITY CRITERIA AND RECRUITMENT

450 The requirements included: age of 25-64 years at the study start, sufficient computer skills and Internet
access via a smartphone compatible with the provided smartwatch; sufficient English language
452 knowledge to be able to understand simple messages and to use health and wellness applications.
We excluded individuals with severe diseases (cancer, cardiovascular, debilitating neurological,
454 psychiatric or orthopaedic diseases). However, individuals with risk factors for chronic diseases (e.g.,

obesity, elevated blood pressure, dyslipidaemias, disturbances in sugar metabolism, mild forms of
456 metabolic syndrome, smoking, moderate drinking or sleep problems) were allowed. Individuals
diagnosed with or suspected of having rare monogenic diseases were excluded. In addition,
458 individuals under custody, with special needs or with limited decisional capacity were excluded, as
well as people suffering from severe forms of alcoholism and depression. Pregnant women were
460 excluded and women becoming pregnant during the study were no longer asked to provide samples
or contribute to the study. Altogether, 645 clients of a private occupational health service (Mehiläinen
462 Töölö, Helsinki, Finland) were invited to participate (Supplementary Figure 1). People interested in
participating (n=125) filled out a questionnaire to assess eligibility. A total of 107 volunteers of
464 European descent from the Helsinki metropolitan area were selected to participate and 96 completed
the study (Supplementary Table 1).

466 *RETURN OF PERSONAL HEALTH DATA*

The ensemble of anthropometrics, clinical laboratory tests, and physiological measurements is called
468 clinical variables in this paper. We returned actionable health data via the Health Dashboard web
application, which allowed participants to: explore and compare their data against reference values
470 and the mean values for the other participants, fill out questionnaires and read informational material.
The clinical variables and their reference values were returned starting at visit 2. A physician interpreted
472 the clinical data and was available to discuss the results with the participants. The occupational health
service communicated any medically-relevant finding requiring immediate actions, while the study
474 group communicated non-acute findings. Clinical decisions were made according to the national
Current Care Guidelines (<https://www.kaypahoito.fi/>). Genetic data were returned to participants under
476 the guidance of a clinical geneticist after visit 2. A personal 10-year risk for coronary heart disease
(CHD) was communicated using KardioKompassⁱ⁴⁴. The risk model is based on both traditional (sex,
478 age, family history, smoking, systolic blood pressure, total and HDL cholesterol) and hereditary risk
factors (approximately 49,000 SNPs). If the risk was >10% the participant was referred to a doctor.
480 We also communicated the risk for low serum 25(OH)D concentration after visit 4 (Sallinen et al., The
Journal of Nutrition, in press). We returned visualizations of questionnaire data on diet, physical

482 activity, sitting, sleeping, subjective health status, and mental wellbeing after visit 4. We also
determined a self-reported obstructive sleep apnea risk score⁴⁵. Participants were able to monitor their
484 physical activity and sleep data using the Withings Health Mate app starting at visit 2.

COACHING AND GROUP MEETINGS

486 Two personal trainers (PTs) coached participants from visit 3 onward. Coaching included nine 30-
minute private meetings (three face-to-face and six remote), email/phone support, as well as group
488 meetings. The PTs were accredited by the European Health and Fitness Association. No structured,
evidence-based coaching protocol was used, but personal actionable possibilities were defined to
490 help participants change their behaviour and improve their health. With the help of a physician and a
nutritionist, the PTs translated and customized actionable possibilities to specific recommendations.
492 The PTs had access to participants' age, clinical variables, fitness test data, and information about
their occupation, exercise, and diet. Tailored health advice and coaching were based on each
494 participant's behaviour, health risks, lifestyle, and goals. One to three relevant, personalized and
actionable opportunities were offered to guide and motivate participants to make lifestyle changes to
496 optimize wellness and health and delay predicted pathologies. Personalized advice usually focused
on diet, exercise, mental wellbeing, or stress and time management. If necessary, a physician limited
498 exercise. Twenty-one informational group meetings were organized during the study, where
participants could interact with a physician, a nutritionist, a nurse, PTs, and other experts. Participation
500 in these meetings was voluntary except for the first, during which a physician and a geneticist
interpreted the clinical variables data as well as the CHD risk prediction.

502 EXPERIMENTAL PROCEDURES

HEALTH CHECK-UP AND CLINICAL VARIABLES

504 Health check-ups occurred on weekdays between 7:30 and noon. Body weight, height, waist and hip
circumferences, blood pressure, and pulse were measured using standard procedures. Participants
506 were asked about medications, dietary supplements, and the use of health care services. Blood and

urine samples were collected at every visit. Fasting (≥ 8 h) blood samples were collected, and clinical
508 chemistry assays were performed on blood, plasma or serum, at the diagnostic laboratory of
Mehiläinen Töölö (Helsinki, Finland), United Medix Laboratories Ltd (Helsinki, Finland) and HUS
510 Diagnostic Center (Helsinki, Finland). Urine samples (≥ 2 h without urinating) were collected using
standard procedures. A dipstick test was performed on the urine samples at the diagnostic laboratory
512 of Mehiläinen Töölö (Helsinki, Finland). Aliquots of blood, plasma, serum and urine were frozen at -
20°C and stored in liquid nitrogen for biobanking.

514 *QUESTIONNAIRE*

Before every visit, participants filled out an online questionnaire, including approximately 150-190
516 questions, depending on the visit, and covering the following: personal information; sociodemographic
and socioeconomic characteristics; familial and individual disease history; functional capacity and
518 health; mental wellbeing; physical activity and exercise habits; diet (including food frequency
questionnaire, FFQ); smoking; alcohol consumption; sleep; occupational health; personality traits;
520 attitudes and expectations towards lifestyle changes; monitoring own health and wellbeing;
expectations towards health technology. Healthy Food Intake Index is a food-based diet quality index,
522 calculated from the FFQ data and adapting an available method⁴⁶.

FITNESS TESTS

524 After every visit, participants were instructed to perform lower-body (squats, repetitions/30s),
abdominal (sit-ups, repetitions/30s) and upper-body (push-ups, max number of repetitions) muscular
526 fitness, balance and mobility tests. Participants executed the tests and uploaded the results to the
Health Dashboard.

528 *ACTIVITY AND SLEEP MONITORING*

After the second visit, participants were equipped with the Withings Activité Pop smartwatch,
530 connected to the Withings Health Mate app, to measure physical activity, energy expenditure and
sleep. Participants were requested to wear the watch until the end of the study. Wellness Warehouse

532 Engine ⁴⁷ embedded in the Health Dashboard was used to authorize and provide the research group
access to participants' data. Only aggregated daily activity and sleep data were exported and included
534 in this study.

SALIVARY CORTISOL

536 Participants collected saliva samples within two weeks of every visit, using Cortisol-Salivette® with a
synthetic swab (Sarstedt). Four samples (awakening, 15 min and 30 min after wake up, bedtime) were
538 collected on a typical weekday. Time and mood at sampling were recorded. Samples were stored at
+4°C until aliquoting and storage at -20°C. Salivary cortisol levels were determined at the University
540 of Trier (Trier, Germany) using a DELFIA immunoassay ⁴⁸. The stress scores derived from the
measurements included: AUCi, AUCg (according to⁴⁹), awakening, evening, peak and Delta (peak -
542 ground) cortisol levels.

DNA EXTRACTION AND GENOTYPING

544 DNA was extracted from whole blood with Chemagic MSM1 (PerkinElmer). Genotyping was performed
at the FIMM Technology Centre (HiLIFE, University of Helsinki, Finland) using InfiniumCoreExome-24
546 v1.0 DNA Analysis Kit, iScan system and standard reagent and protocols (Illumina). Genotypes were
pre-phased with ShapeIT2 and imputed with IMPUTE2. Two pre-phased reference panels were used
548 (--merge_ref_panels): 1000G Phase 1 and a Finnish low-coverage WGS imputation reference panel,
composed of 1,941 whole-genome sequences (SISu project). Imputation resulted in 30.3 million
550 quality-filtered variants ($R^2 > 0.3$ and missingness < 0.05).

GCMS AND LCMS

552 GCMS and LCMS experiments were performed at the Swedish Metabolomics Center (Umeå). 100 µl
of plasma were processed as described⁵⁰, with the following details: extraction with 900 µl of 90% v/v
554 methanol, containing internal standards for both GCMS and LCMS, at 30 Hz for 2 minutes; protein
precipitation at +4 °C; centrifugation at +4 °C, 14 000 rpm, 10 minutes. 50 or 200 µl of supernatant
556 were evaporated to dryness in a speed-vac concentrator, for GCMS or LCMS analysis respectively,

and stored at -80 °C. Quality control (QC) samples were created by pooling supernatants. MSMS
558 analysis (LCMS) was run on the QC samples for identification purposes. Sample batches were created
according to a randomized run order. For GCMS, derivatization and analysis were performed as
560 described previously⁵⁰, with the following modifications: 0.5 µL of derivatized sample; splitless injection
with a L-PAL3 autosampler (CTC Analytics AG); 7890B gas chromatograph (Agilent Technologies);
562 chemically bonded 0.18 µm Rxi-5 Sil MS stationary phase (Restek Corporation); column temperature
increased from 70 to to 320 °C at 40 °C/min; Pegasus BT TOFMS (Leco Corporation); solvent delay of
564 150 s; detector voltage 1800-2300 V. Unprocessed MS-files were exported from the ChromaTOF
software in NetCDF format to MATLAB R2016a (Mathworks), where processing occurred, including
566 baseline correction, chromatogram alignment, data compression and Multivariate Curve Resolution.
The extracted mass spectra were identified by comparisons of their retention index and mass spectra
568 with known libraries using the NIST MS 2.0 software⁵¹. Annotation was based on reverse and forward
searches in the library. LCMS experiments were performed as described⁵² and all data processing was
570 performed using the Masshunter Profinder version B.08.00 (Agilent Technologies). The processing was
performed both in a target and an untargeted fashion. For target processing, a predefined list of
572 metabolites commonly found in plasma and serum were searched for using the Batch Targeted feature
extraction in Masshunter Profinder. An-in-house LCMS library, built up by authentic standards run on
574 the same system with the same chromatographic and MS settings, was used for the targeted
processing. The identification of the metabolites was based on MS, MSMS and retention time
576 information.

AUTOANTIBODY BEAD ARRAYS

578 Autoantibody profiling on antigen bead arrays was performed as previously described²⁷, at the
Autoimmunity and Serology Profiling facility at SciLifeLab (Stockholm).

580 *PEA*

Plasma proteins were quantified using Proximity Extension Assay (PEA) at Olink Bioscience (Uppsala),
582 using 6 panels: Cardiometabolic, CVD II, CVD III, Inflammation I, Metabolism and Oncology II. Each

panel assayed 92 proteins using a matched pair of antibodies coupled to oligonucleotides, which form
584 an amplicon by proximity extension and can be quantified by real-time PCR. The data were normalized
against an extension control and an interplate control and expressed as Normalized Protein
586 eXpression (NPX) values, which represent an arbitrary relative quantification unit on log₂ scale. The
NPX values below the limit of detection (LOD) were considered missing and their value was replaced
588 with the LOD value for each assay.

MICROBIOME ANALYSIS

590 Participants collected faecal samples within two weeks of every visit. Samples were collected in
precooled vials placed in styrofoam boxes with ice gel packs and then stored at +4°C for a maximum
592 of one day until aliquoting, freezing at -20°C, and storage in liquid nitrogen without additives. Thawed
faecal samples were spun-down and DNA was extracted, with 50 ng of DNA submitted to PCR
594 amplification as described⁵³, using 341f and 805r primers (CCTACGGGNGGCWGCAG and
GTGBCAGCMGCCGCGGTAA) for the V3–V4 regions of 16S rRNA⁵⁴. Sequencing was done on an
596 Illumina MiSeq with 2x250 bp reads. After quality trimming with Cutadapt, an ASV (amplified sequence
variants) table was generated using the DADA2 pipeline⁵⁵, including the following steps: filtering and
598 trimming, learning of error rates, dereplication, sample inference, read pairs merging, removal of
chimeras and taxonomy assignment using SILVA v128 database.

600 *BIOINFORMATIC ANALYSES*

LONGITUDINAL ANALYSIS

602 We applied Generalized Estimating Equations (GEE) to the quantitative clinical variables to investigate
the longitudinal changes while controlling for sex and age. As data feedback and coaching started
604 respectively from visit two and three, we excluded the first visit and considered the second visit as
baseline. Four time points (0-4) were then considered and we aimed at extracting the average change
606 per visit, assuming the same change in the values between any two successive visits. Furthermore,
for each variable, individuals were classified as Out-Of-Range at Baseline (OORB) if the values were

608 outside the reference range (Supplementary Table 2) at baseline. We assumed that the longitudinal
changes could be distinct for individuals classified as ORRB. In other words, we allowed the effect of
610 coaching and data feedback to be different in the two groups by introducing an interaction term. If the
ORRB group included at least five individuals, then the variable was modelled as:

612 $\text{value} \sim \text{Sex} + \text{Age} + \text{Time.point} + \text{ORRB} + \text{Time.point:ORRB}$

Otherwise, a model with no groups of individuals was considered:

614 $\text{value} \sim \text{Sex} + \text{Age} + \text{Time.point}$

GEE models were fitted using the `geepack` library and exchangeable correlation structure. We
616 extracted the effects, their standard errors and p-values using the `esticon` function in the `doBy`
library. If no interaction was specified, the coefficient for `Time.point` represented the estimated change
618 for all the individuals, expressed as the change occurring between two successive visits. If the
interaction was included, we considered the change occurring in the ORRB group between two
620 successive visits, and we extracted the effect as the linear combination of the coefficients of
`Time.point` and `ORRB`. P-values were adjusted with the Benjamini-Hochberg method. Model
622 prediction of the variable values was visualized by stratifying for sex and ORRB group. The 95%
confidence levels were estimated by bootstrapping with 1000 replications.

624 *DIMENSIONALITY REDUCTION*

We selected the quantitative clinical variables and imputed missing using the `imputePCA` function in
626 the `missMDA` package. Principal Component Analysis (PCA) was performed with the `PCA` function in
the `FactoMineR` package on scaled data. Variable contribution to a given PC was defined as the ratio
628 between the squared cosine of a variable and the sum of the squared cosines for all the variables for
that component.

630 *DATA PREPROCESSING*

632 *Activity and sleep.* We obtained summary measures for the activity and sleep data by calculating average values for the different variables in the previous 30 days before each visit. We considered only samples for which at least 10 days were included in the calculation.

634 *GCMS.* The relative quantities (RQs) were log₂-transformed and missing values were imputed with the KNN algorithm. Data were normalized using the RUV4 method in the `ruv` R library⁵⁶. RUV4 was applied
636 to remove sources of technical variability, including batch effect and the signal drift over time. Briefly, we used the internal standards (IS) as negative controls, $k=4$ and a design matrix with individuals and
638 visits as covariates, in order to estimate the matrix W of unwanted factors and their respective α coefficients. The number of factors to remove (k) was chosen with the `getK` routine, but was ensured
640 not to exceed 1/3 of the number of the IS. The normalized relative concentrations were obtained by subtracting the effect of the W components from the RQs. The IS values were inspected before and
642 after normalization to ensure a removal of the signal drift over time and a reduction of the Coefficient of Variation (CV). Estimation of the Intraclass Correlation Coefficient (ICC) and PCA plots were also
644 evaluated to inspect the performance of the normalization method.

LCMS. The negative and positive modes from LCMS experiments were processed separately.
646 Unidentified metabolite peaks and metabolites with more than 25% of missing data were removed. RQs were log₂-transformed and missing values were imputed with KNN. RUV4 adjustment and
648 inspection of the results were performed as described above with $k=2$ or $k=1$ for LCMS-neg and LCMS-pos data, respectively.

650 *Autoantibodies.* We considered: continuous Median Fluorescence Intensity (MFI), discrete binned and binary (0=undetected, 1=detected) data (see²⁷). MFI values were normalized with the Probabilistic
652 Quotient Normalization⁵⁷, with a median reference profile, and then log₂-transformed.

16S rRNAseq. The ASV count table represents an analog of the traditional Operational Taxonomic Unit
654 table. We inspected the taxa prevalence (the number of samples in which a taxon has nonzero counts) and the total abundance (sum of the counts in all samples) and the abundance distribution. Using
656 phyloseq, we agglomerated the counts to the genus level, to reduce functional redundancy. The

genus-level data were filtered to remove taxa with missing phylum annotation, prevalence ≤ 2 and total
658 abundance ≤ 10 . We inspected the ordination of the samples using several distance metrics. We then
converted the genus-level count to a DESeq2 dataset and used the Variance Stabilizing
660 Transformation (VST), which normalizes with respect to the library size and gives a matrix of
approximately homoscedastic values that can be used for downstream analyses. As a major source
662 of batch effect was represented by the experimental plate, we verified that the VST conversion also
reduced the library size effect by visualizing the sample ordination, using MDS with Bray-Curtis
664 distance for the genus-level counts and Euclidean distance for the VST values. We also formally tested
the reduction of the batch effect, by looking at the association between the first two axes of the sample
666 ordination plots with the plate ID. The estimation of the α -diversity for each sample was done using
the original unfiltered counts.

668 *INTEGRATION OF MULTIOMICS EXPERIMENTS*

A MultiAssayExperiment object was assembled with all the continuous clinical and omics data, namely
670 RUV4-normalized data for GCMS, LCMS-neg and LCMS-pos, log₂MFI for autoantibodies, NPX values
for PEA assays and VST-transformed values for 16S counts. Data filtering to remove unwanted
672 features included: removal of internal standards from GCMS and LCMS; removal of proteins NPX
values < LOD (i.e. missing data) in more than 25% of the samples; removal of FS, CCL22 and BDNF
674 (technical issues, Olink communication); removal of autoantibodies with background fluorescence in
all samples (scored reactivity values ≤ 0.5); removal of bacterial taxa with a prevalence $\leq 30\%$. We used
676 the filtered object for all the downstream analyses. The resulting dataset included 136 GCMS
metabolites, 104 LCMS-neg metabolites, 163 LCMS-pos metabolites, 174 autoantibodies, 501
678 proteins and 85 bacterial taxa (Supplementary table 2).

VARIANCE PARTITION ANALYSIS

680 For each omics type, between- and within-individual variation was inspected with a distance-based
method and with variance partitioning analysis. For the distance method, Euclidean distance between
682 all pairs of samples was calculated. Then, the within-individual distance was calculated as the median

value of the distance values of the sample pairs from the same individual. This value was plotted
684 together with the distribution of the remaining distance values, i.e. the distances between one
individual and the rest of the individuals. For the variance partitioning method, a linear mixed model
686 was fitted with lme4 R library, independently to each feature with nonzero variance. We included the
individual as a random intercept and age, sex and time point (0-4) as fixed effects. The fixed effect
688 variance, random intercept variance and residual variance components were extracted and the relative
fraction calculated. The random intercept variance represented the between-individual variance, while
690 we interpreted the residual variance as the within-individual variance not accounted by the fixed
effects.

692 *MULTI-OMICS FACTOR ANALYSIS*

Multi-Omics Factor Analysis v2 (MOFA+) provides a set of factors that capture biological and technical
694 sources of variability^{11,12}. It infers the axes of heterogeneity that are shared across multiple modalities
and those specific to individual data modalities. We used the “intercept_factor” branch of the code
696 repository (https://github.com/bioFAM/MOFA2/tree/intercept_factor). For training, we selected the
samples that had a measurement in all the omics layers (n=359). We considered a Gaussian likelihood
698 for the continuous measurements for all the layers, except for autoantibodies, which were considered
in their binary form (0=undetected, 1=detected) with Bernoulli likelihood. Data were not scaled. We
700 trained 10 alternative models in Python with a random seed, starting from 20 factors and the following
options: iter=”10000”, convergence_mode=”medium”, dropR2=”0.02”. The model with the best value
702 of the Evidence Lower Bound (ELBO) was selected. We checked the robustness of the learned factors
by inspecting the Pearson correlation between the factors obtained by all the runs (Supplementary
704 Figure 6). We then computed the fraction of the total variance explained by each factor and the fraction
of variance explained by each factor in each layer. We inspected the factor loadings to understand the
706 contribution of the original features. A feature with a higher absolute loading has a higher weight on
the factor, but because the loadings are not directly comparable, their scaled values were used for
708 visualization. The sign of the loading defines a direct (positive) or inverse (negative) proportionality with

the corresponding factor, and features with similar loadings contribute similarly to the factor. We
710 inspected the factor values and to visualize and cluster the samples on the reduced space.

ASSOCIATION BETWEEN FACTORS AND PHENOTYPIC VARIABLES

712 In order to test the association between the MOFA+ factors and the sample characteristics, we
gathered a collection of phenotypic information including: clinical variables; questionnaire data (family
714 history, exercise and physical activity, functional capacity and health, mental health, diet, smoking,
alcohol use and sleep habits); Healthy Food Intake Index; KardioKompassi risk; sleep apnea score;
716 stress scores; fitness tests; sleep and activity summaries from the wearables. For each combination
of factor and phenotypic variables, we fitted a linear model with the factor values as outcome and the
718 phenotypic variable as predictor. Reported R^2 values were derived from these models. For the
categorical variables, the predictor was considered an ordered factor if the factor levels corresponded
720 to ordered levels and the variable could be considered as a qualitative or semi-quantitative ordinal
variable. A False Discovery Rate (FDR) was calculated using the Benjamini-Hochberg method. The
722 candidate associations for further screening were obtained at $FDR < 0.05$, while the associations
reported in Figure 3 satisfy a $FDR < 0.001$ threshold, in order to better control for false positives arising
724 from the multiple hypotheses tested. The selected associations were refined with linear mixed models
as implemented in lme4 library. We modelled the LF values with the individual as a random intercept
726 and age and sex as fixed effect. We refer to these models as the covariate-adjusted models. P-values
for these models were obtained with the “Type II ANOVA” as implemented in the `Anova` function in
728 the car library, with a Kenward-Roger F test.

POPULATION STRATIFICATION

730 The DHR and the 1000 Genome phase 3 genotypes were merged. Analyses were done with PLINK
v1.9. Only autosomal biallelic SNPs with genotyping rate $>95\%$ and $MAF > 5\%$. were considered. A set
732 SNPs in approximate Linkage Disequilibrium was obtained with the option `--indep-pairwise 50 5 0.2`
and PCA was performed. To predict the ethnicity, a Linear Discriminant Analysis model (`lda` in MASS)
734 was trained in R with the PCA scores of the 1000 Genomes only and tested on the DHR samples.

GWAS SUMMARY SCORES

736 We considered 146 traits from the GWAS catalog v1.0.1 (<https://www.ebi.ac.uk/gwas/>) for selected
ontology categories: body measurement, cardiovascular disease, cardiovascular measurement,
738 hematological measurement, inflammatory measurement, lipid or lipoprotein measurement, liver
enzyme measurement, metabolic disorder and other (fasting blood glucose, vitamin D levels and
740 thyroid stimulating hormone). For each trait, only the studies meeting the following criteria were
considered: at least one SNP with $p\text{-value} < 1E-08$, sample size > 5000 , at least 10 SNPs reported. The
742 study with the largest sample size was considered for the traits with multiple associated studies. For
each biallelic SNPs, the reported effect size of the risk allele was considered as a weight. Summary
744 scores were computed by multiplying the imputed genotype dosage of each risk allele times its
respective weight and summing across all SNPs.

746 *BETWEEN- AND WITHIN-INDIVIDUAL CROSS CORRELATION NETWORK*

We considered the continuous measurements for all the omics layers, together with a collection of
748 measurements including: GWAS summary scores; gut microbiome alpha diversity; clinical variables;
questionnaire data; Healthy Food Intake Index; KardioKompassi risk; sleep apnea score; stress scores;
750 fitness tests; sleep and activity summaries. The resulting dataset was preprocessed by regressing out
the effect of sex and then the effect of age for each variable, only if significantly associated. For the
752 between-individual cross correlation network calculation, the observations were grouped by individual
and averaged, obtaining 96 independent observations for each of the 1394 variables. Spearman
754 correlation was calculated for each pair of variables, resulting in 731318 nonmissing estimated ρ
coefficients, p -values and Benjamini-Hochberg adjusted p -values (FDR), for the pairs of features of
756 different types (activity and sleep, autoantibody, clinical variables, fitness test, genetic, HFII,
KardioKompassi, metabolite, microbial, protein, sleep apnea score, stress score). For the within-
758 individual cross-correlation network calculation, the GWAS scores and the autoantibody data were
excluded, resulting in 1058 variables, 96 individuals and 5 time points. We used `rmcorr` library⁵⁸ to
760 estimate the common within-individual association for grouped values measured at the five visits.

`rmcorr` estimates a common regression slope representing the association shared among individuals

762 and provides the best linear fit for each individual using parallel regression lines with different
intercepts. The repeated-measures correlation coefficient (r_{rm}) is similar to the Pearson correlation
764 coefficient and measures the strength of a linear association but, unlike Pearson correlation, it takes
into account non-independence between the measures. Hence, we estimated 347640 nonmissing r_{rm} ,
766 p-values and Benjamini-Hochberg adjusted p-values (FDR), for the pairs of features of different types
and with at least 100 nonmissing pairs of values. For downstream analysis, we selected the
768 associations satisfying the condition $FDR < 0.05$ and $coefficient > 0.3$ (ρ or r_{rm}), and generated two
annotated correlation networks. Communities were extracted with the Louvain method, resulting in
770 modularity values of 0.70 and 0.69 for the between- and within-individuals correlation network
respectively.

772

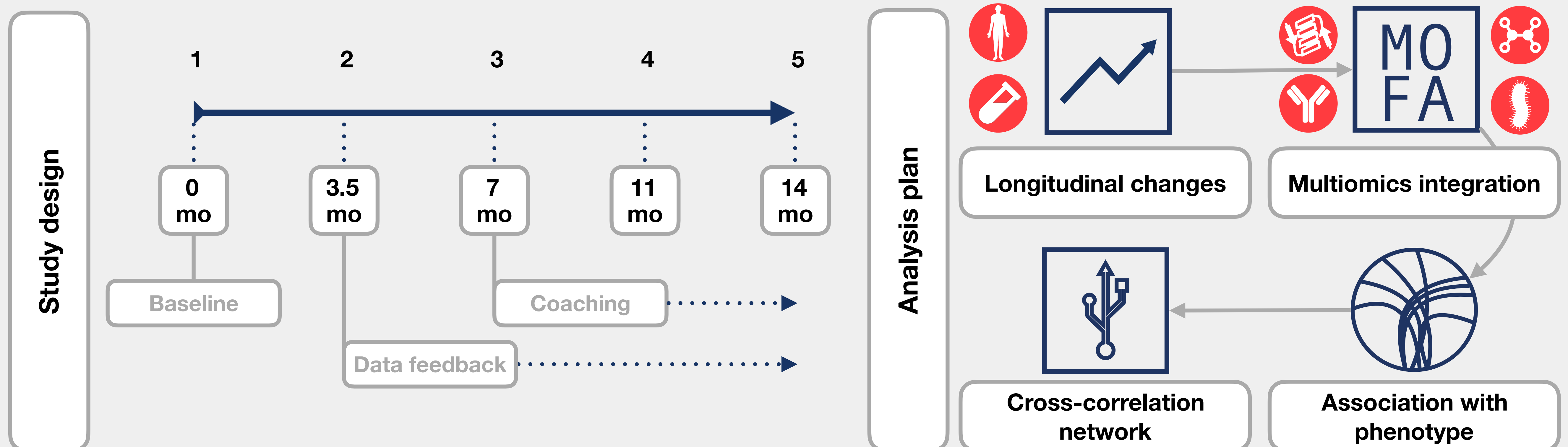
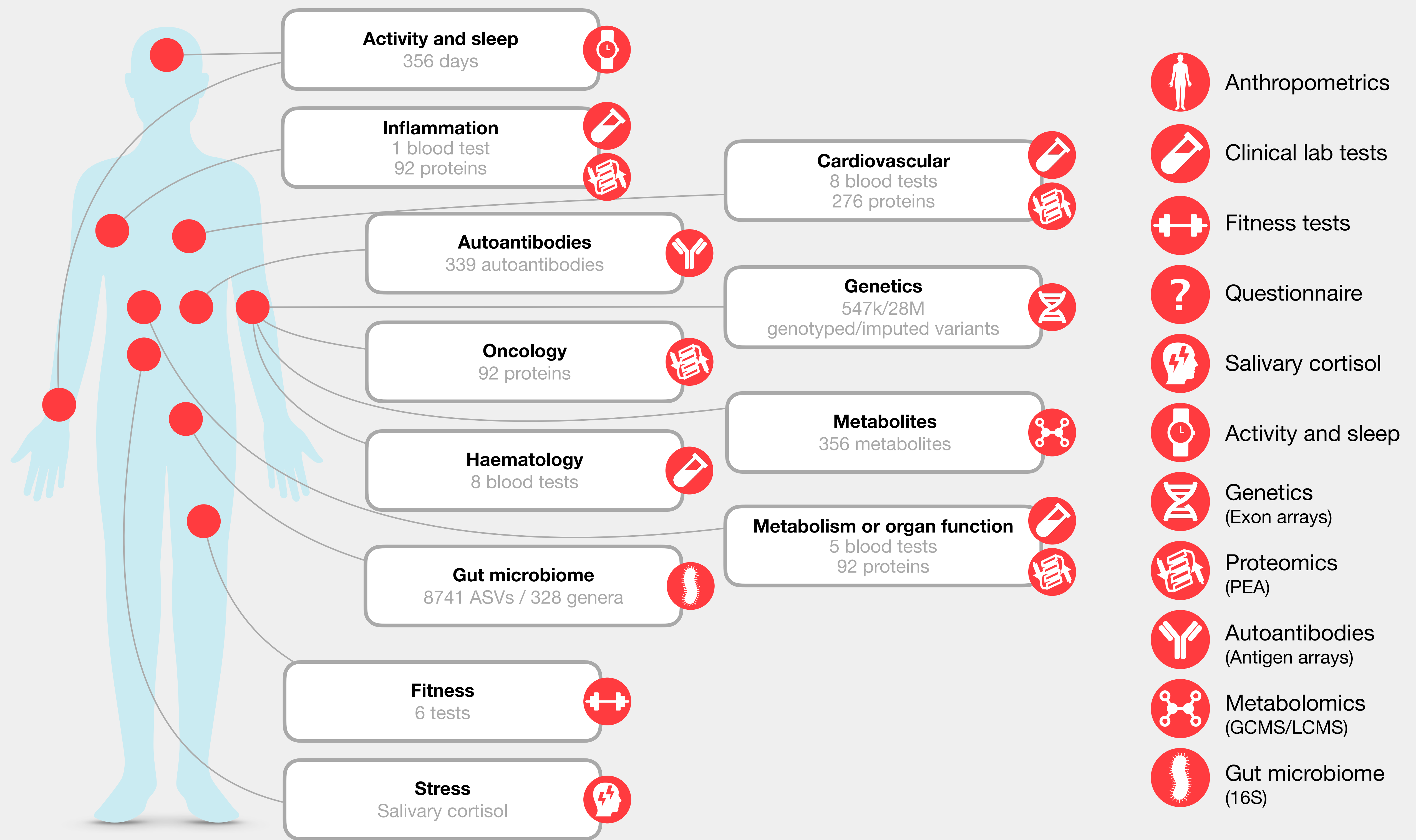
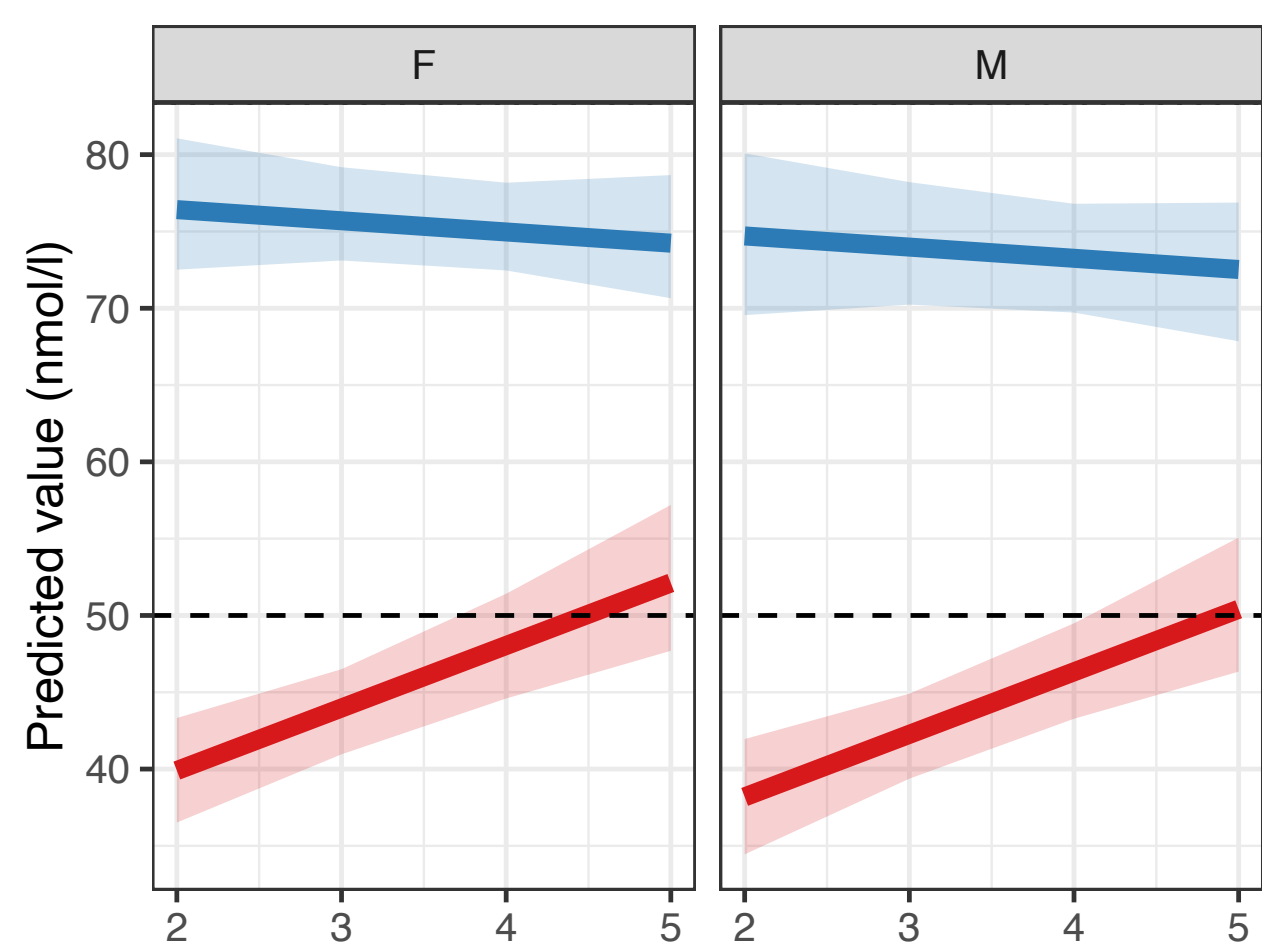
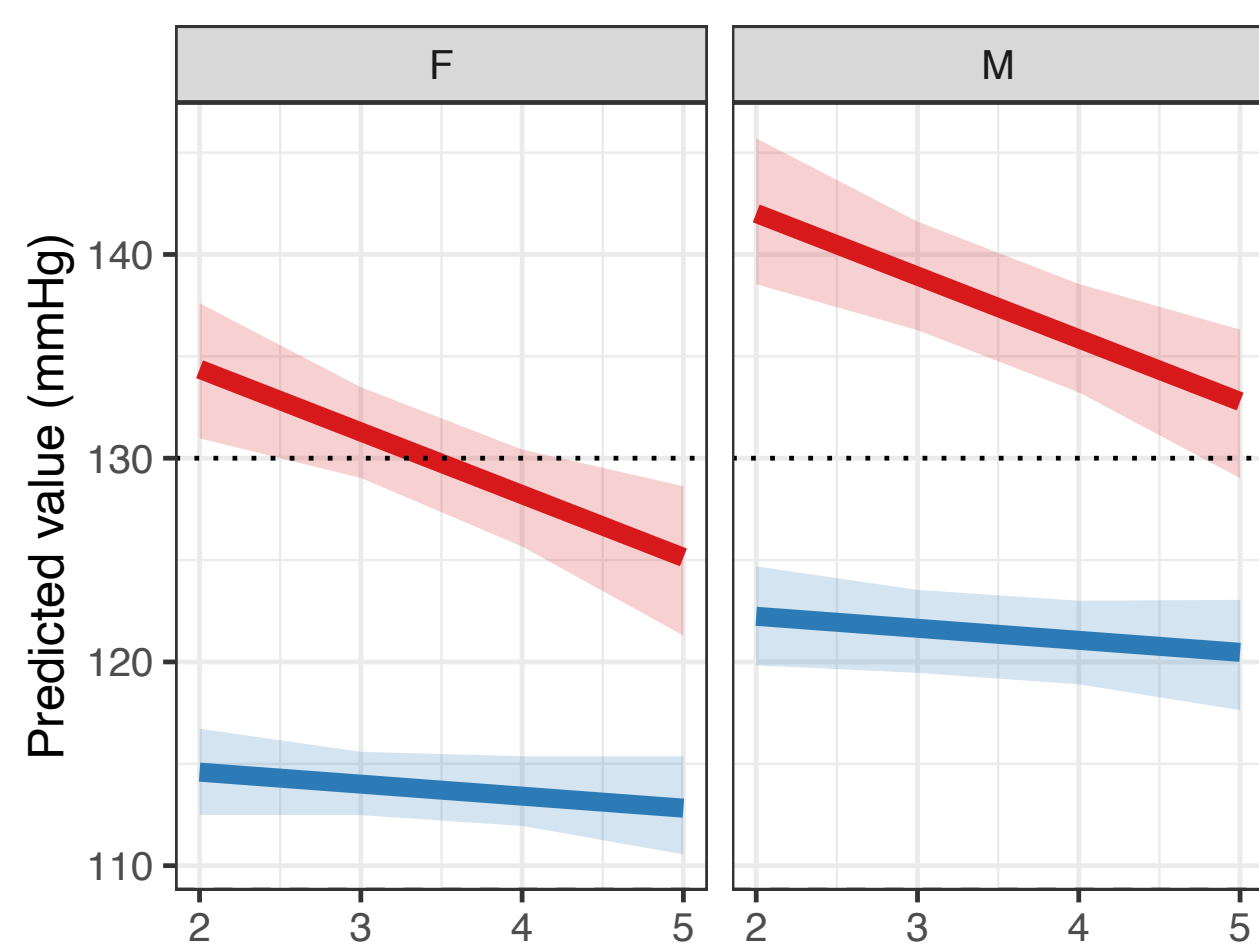
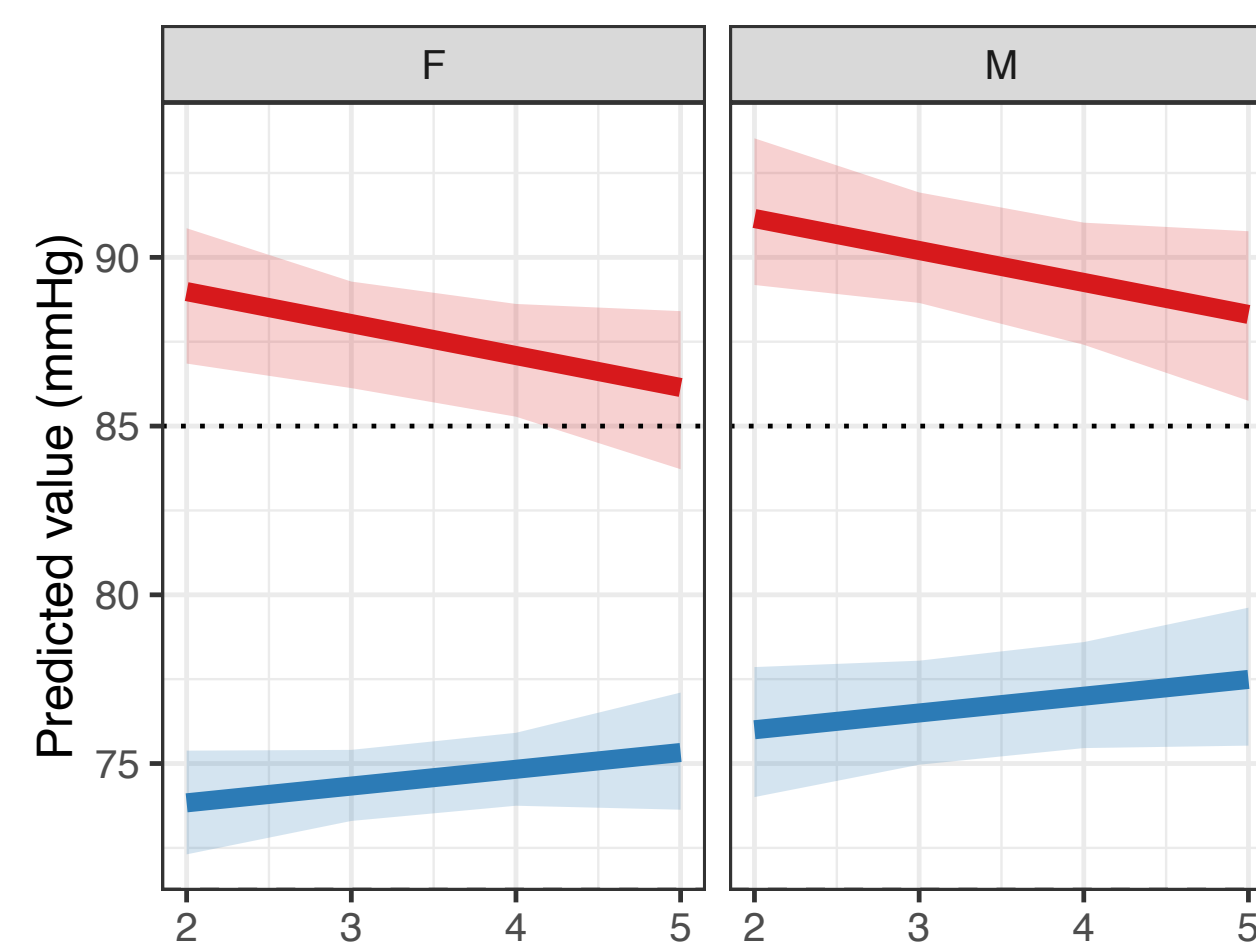
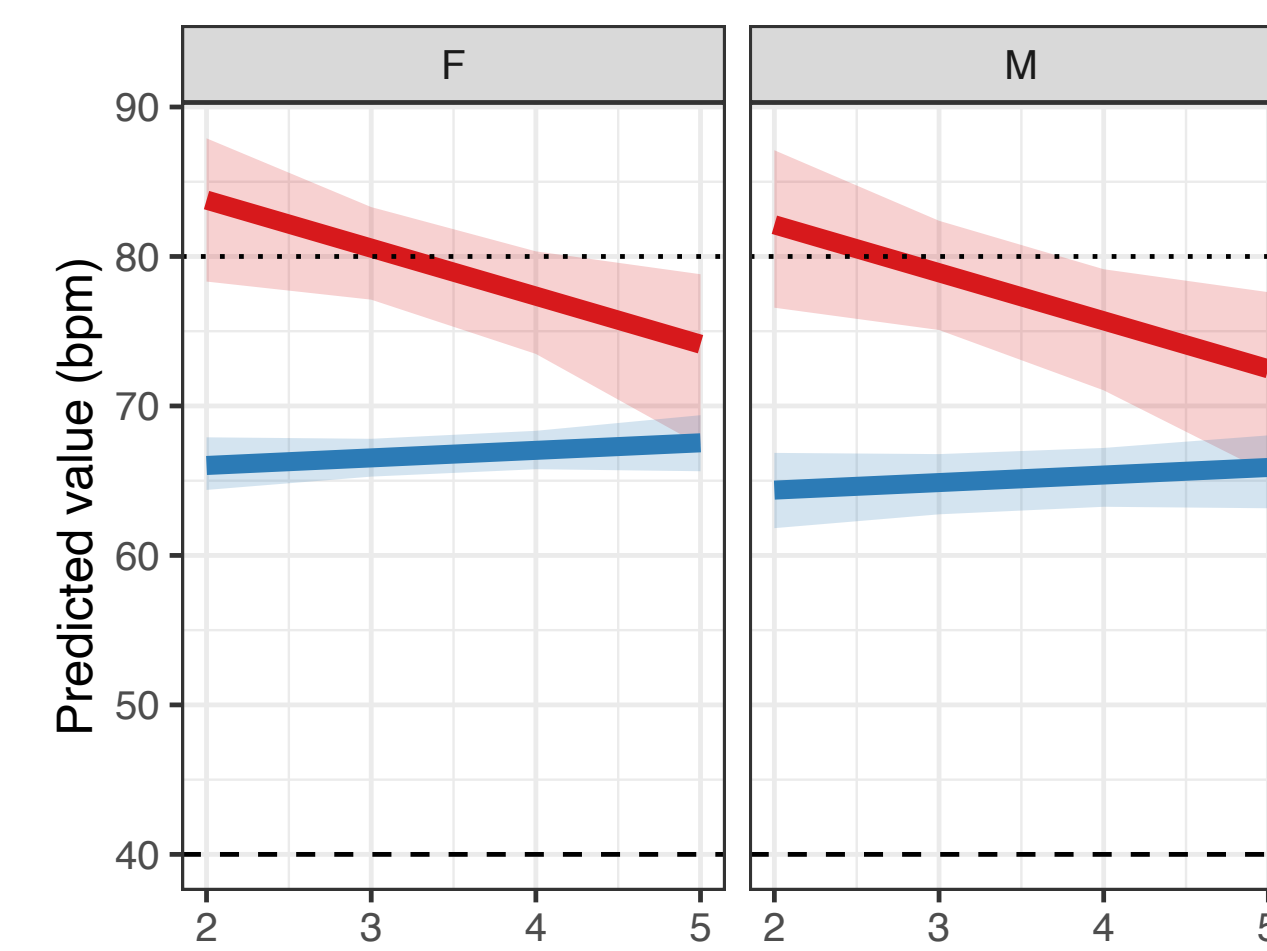
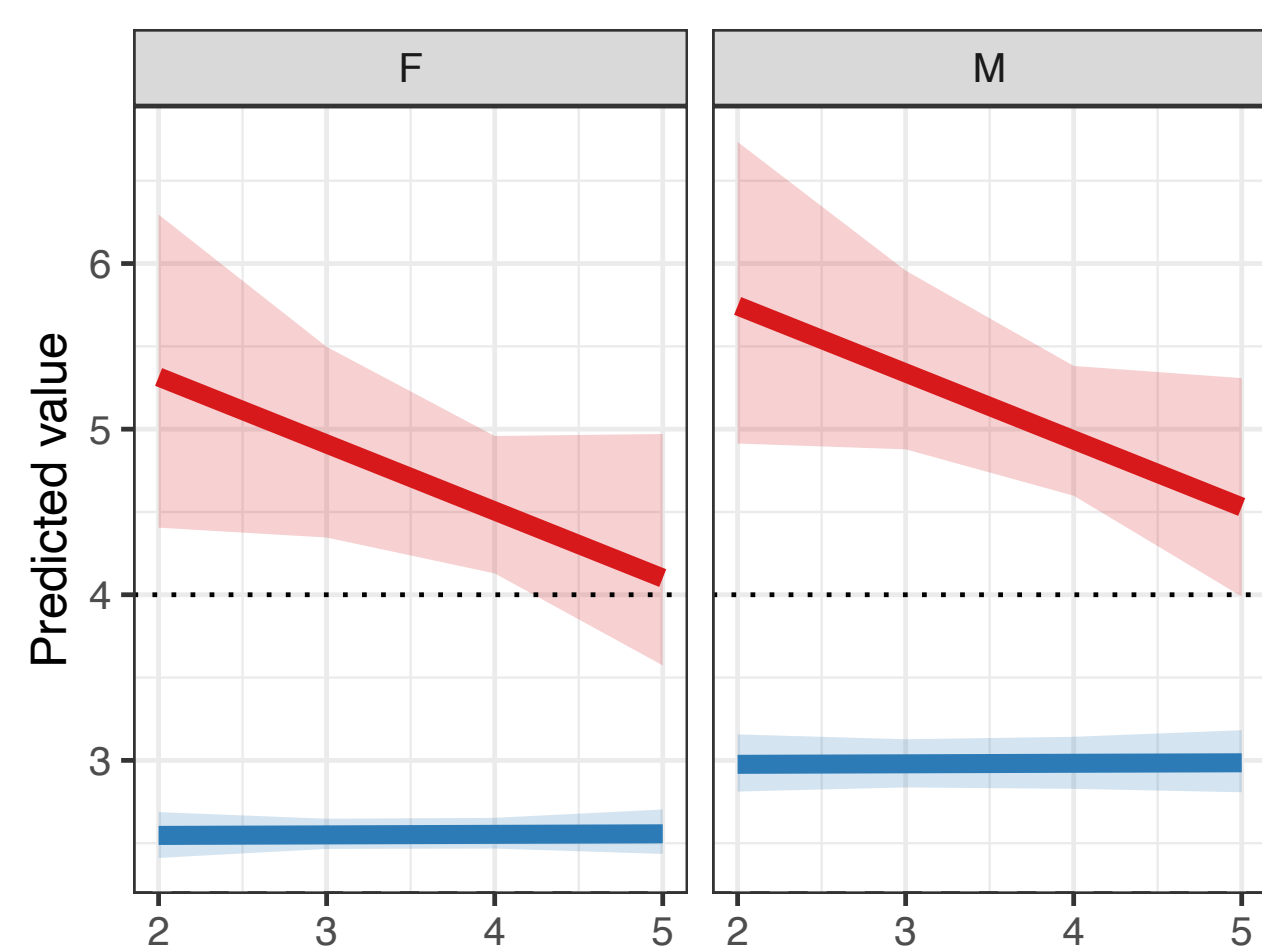
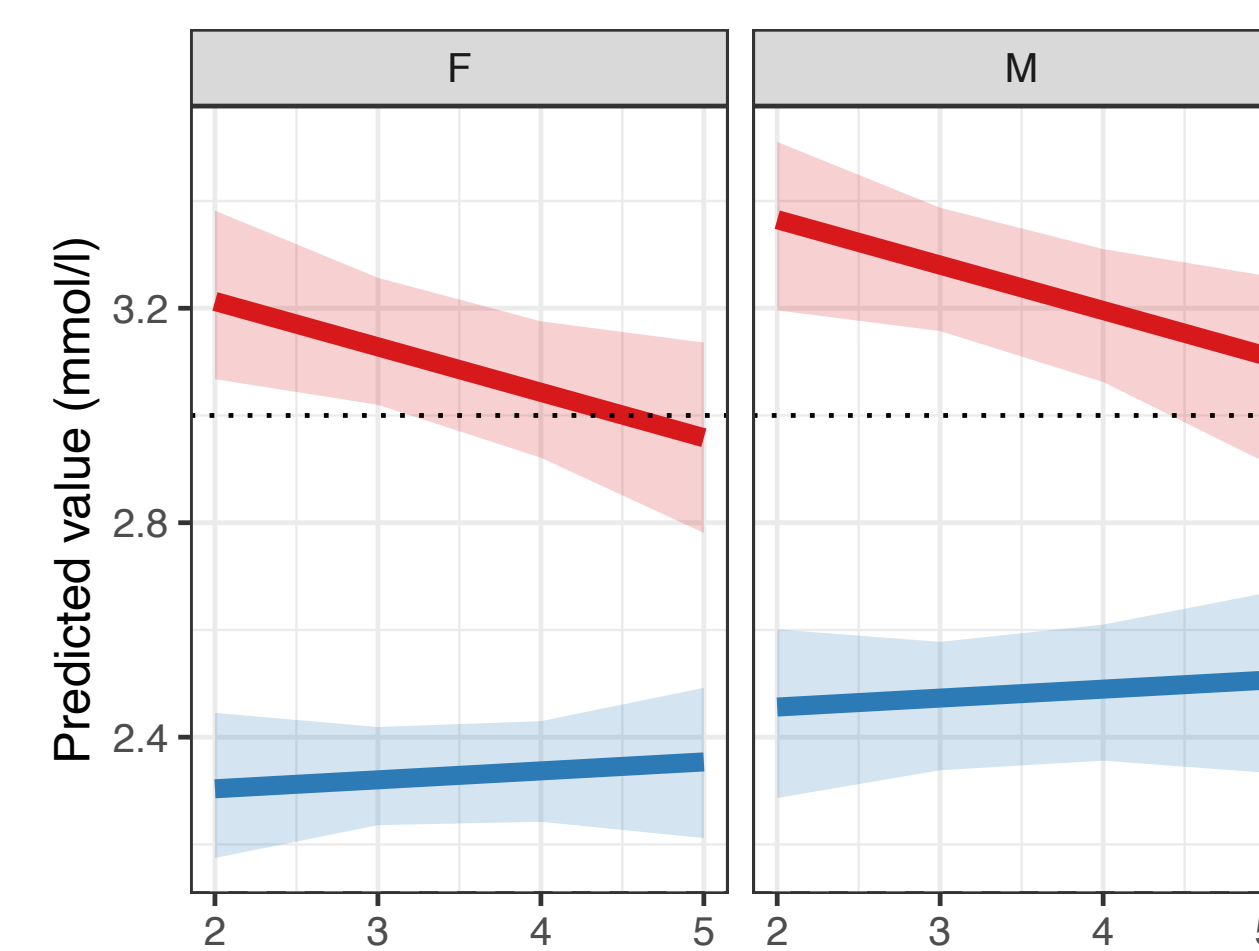
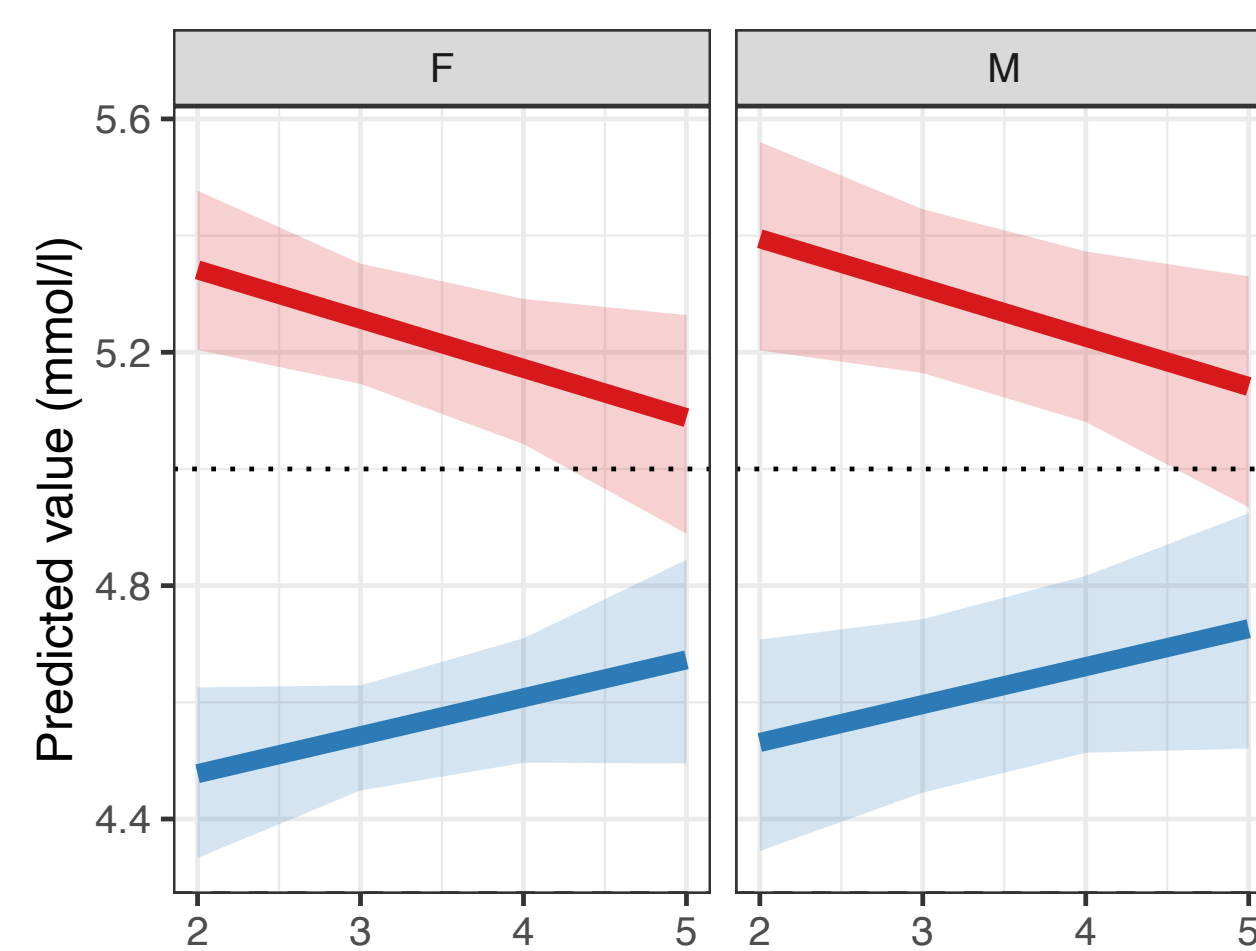
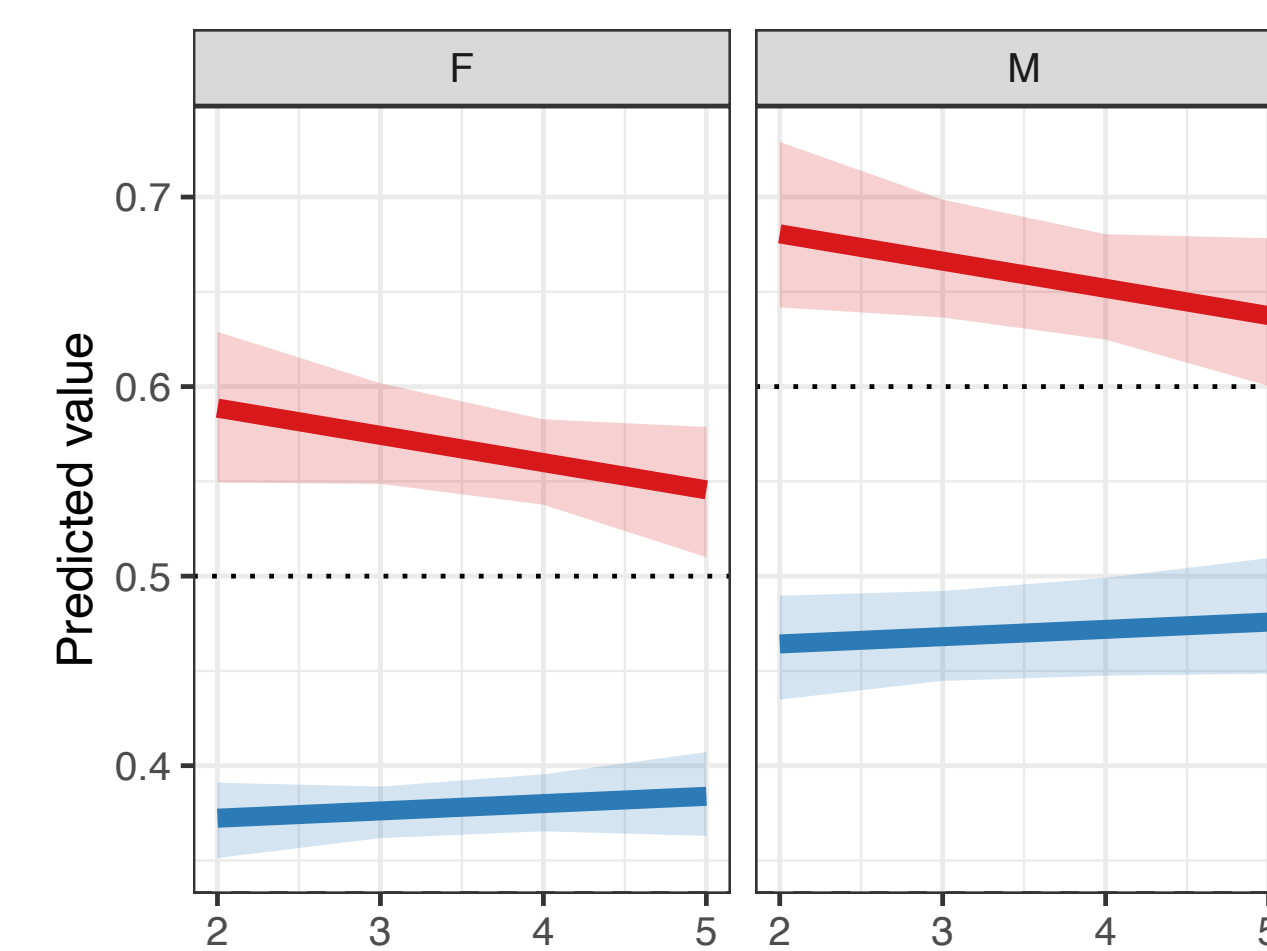
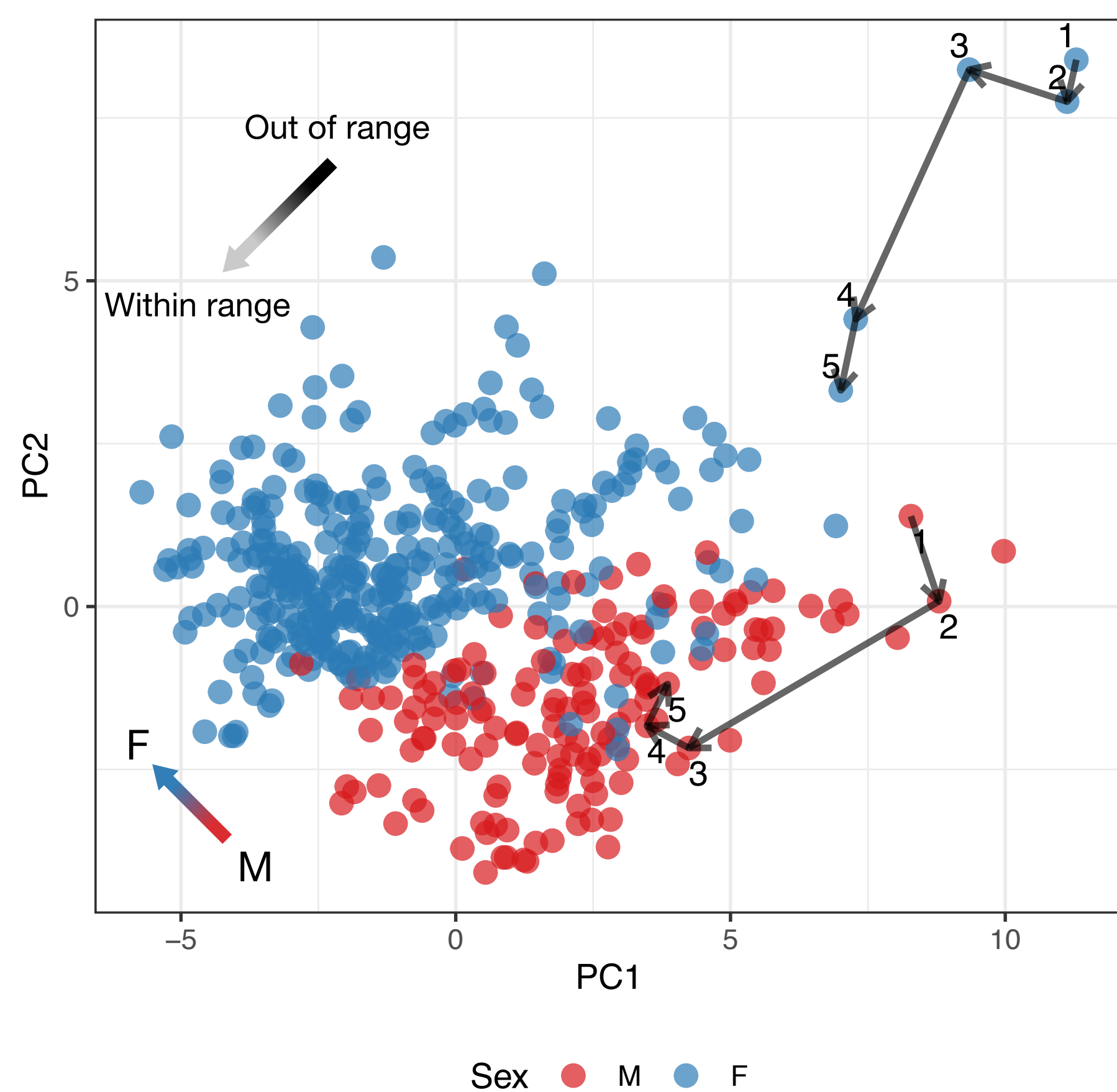
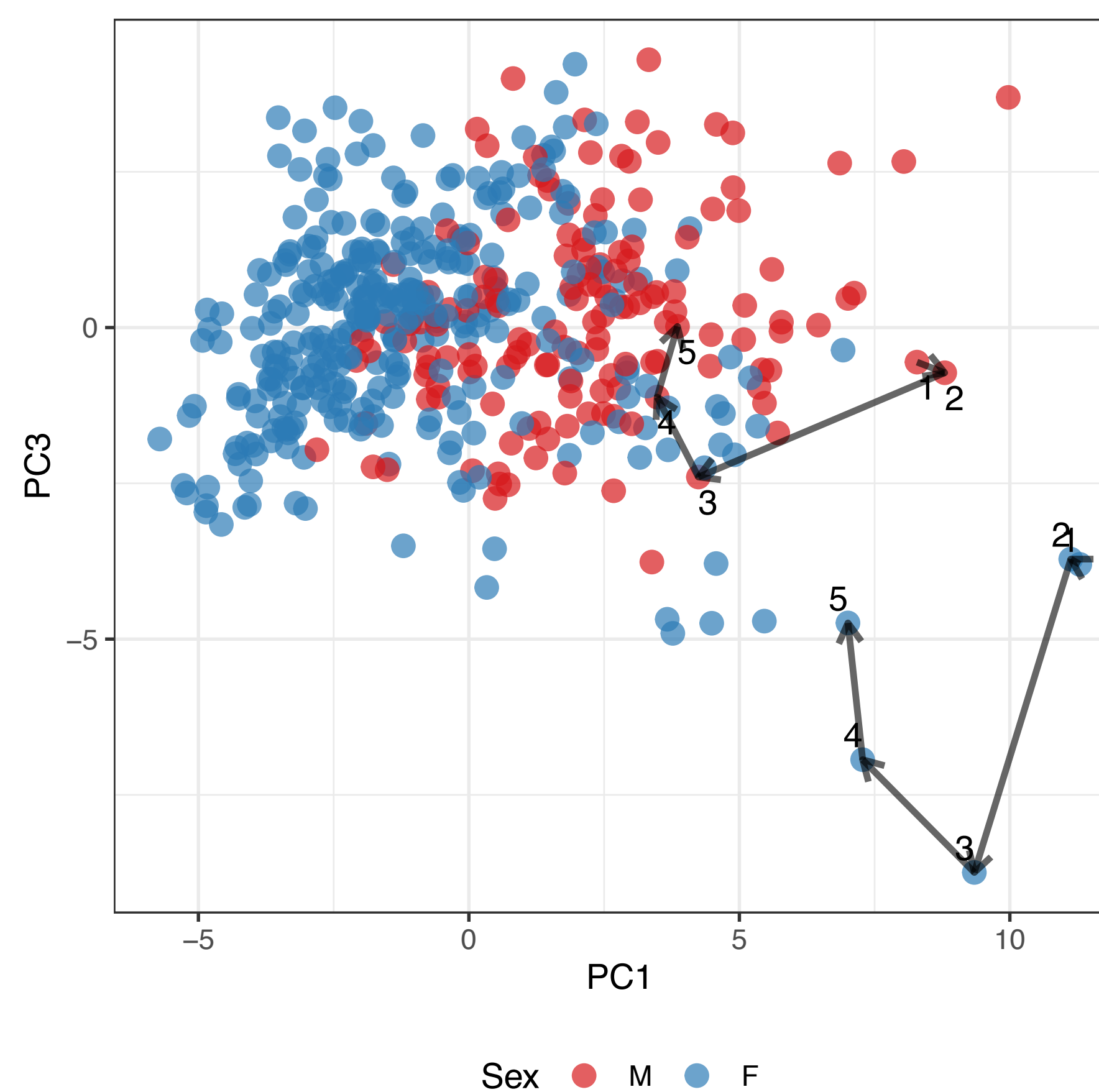
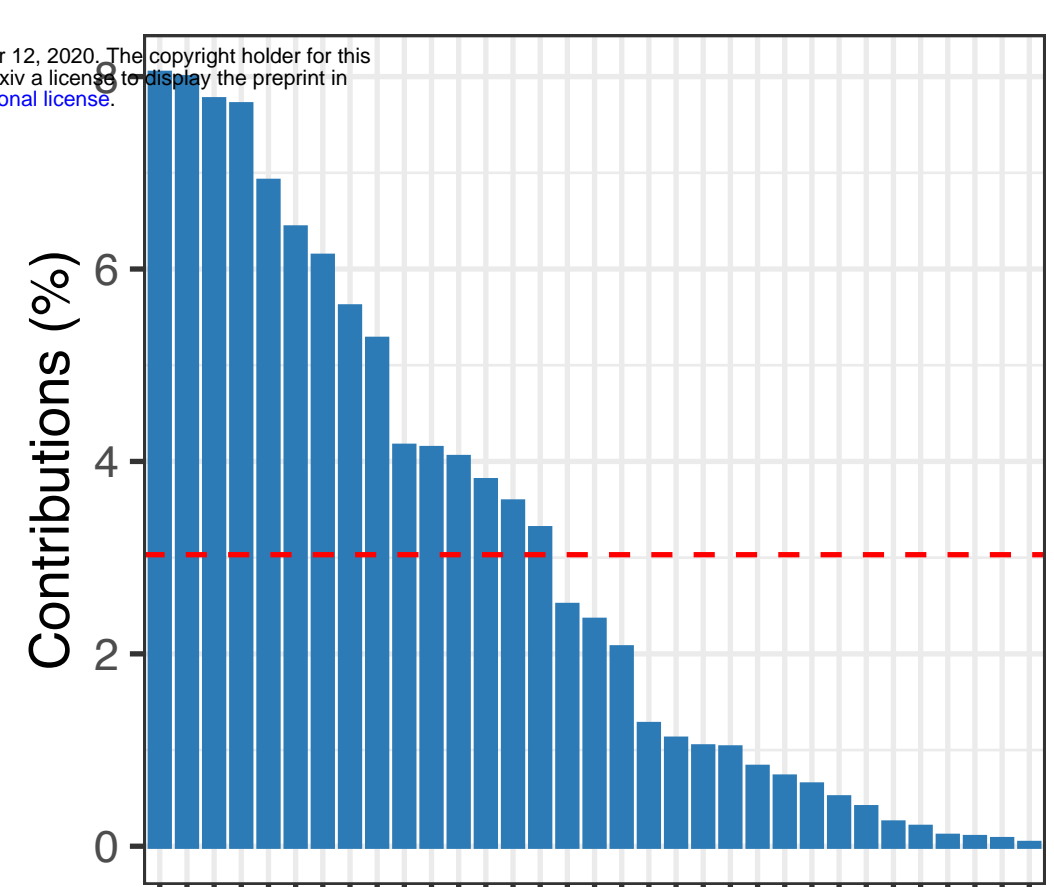


Figure 2: Overview of the measured features, longitudinal design and analysis workflow.

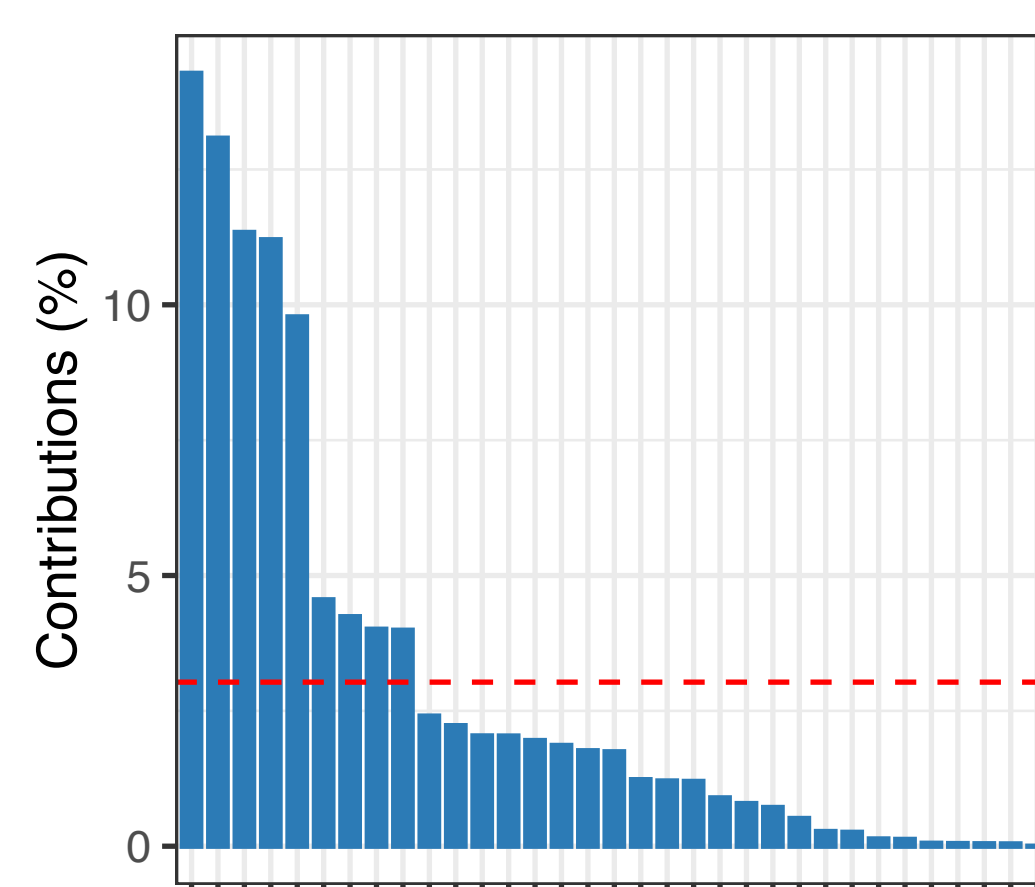
A**25(OH)D (Vitamin D)**Initial value ■ Out of range ■ Within range**Systolic blood pressure**Initial value ■ Out of range ■ Within range**Diastolic blood pressure**Initial value ■ Out of range ■ Within range**Pulse**Initial value ■ Out of range ■ Within range**Total chol./HDL chol. ratio**Initial value ■ Out of range ■ Within range**LDL cholesterol**Initial value ■ Out of range ■ Within range**Cholesterol**Initial value ■ Out of range ■ Within range**ApoB/ApoA1 ratio**Initial value ■ Out of range ■ Within range**B**Sex ● M ● FSex ● M ● F

PC1



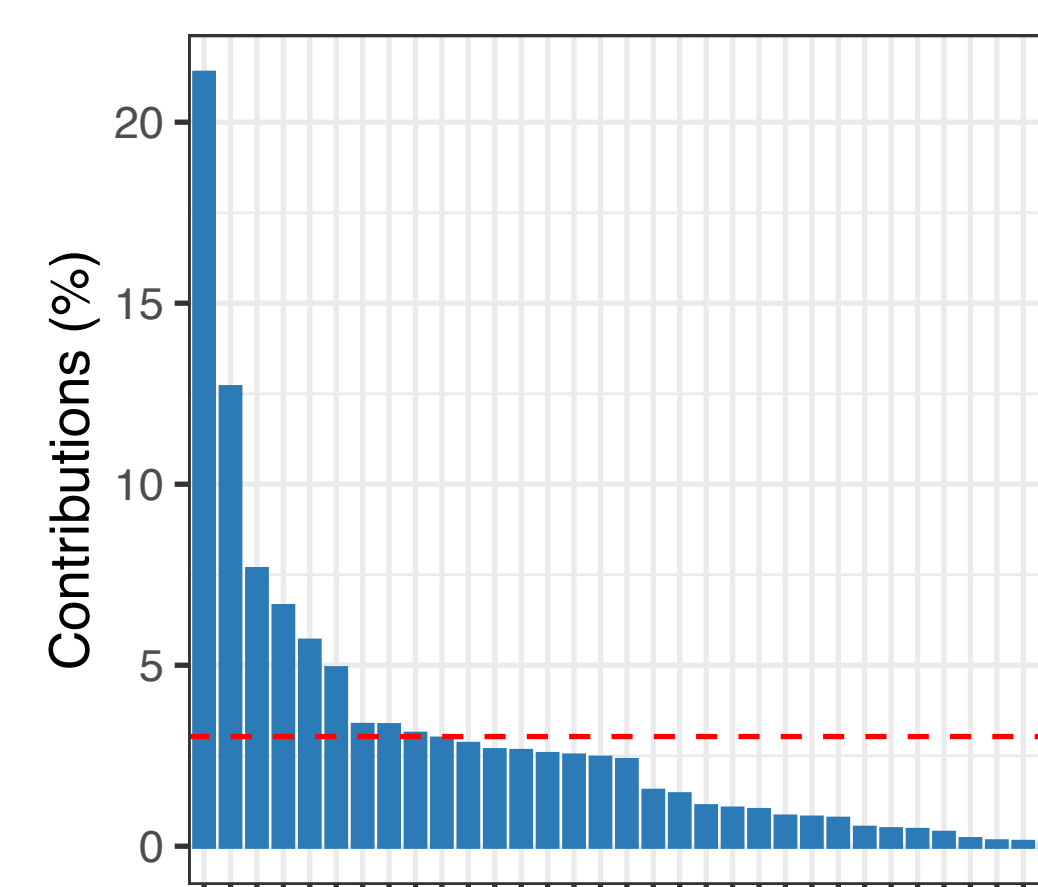
ApoB-ApoA1 ratio
Waist
Total chol./HDL chol. ratio
Weight
BMI
ApoB
Hip
HDL cholesterol
Triglycerides
LDL cholesterol
Glucose
Erythrocytes
Haemoglobin
Haematocrit
Insulin

PC2



Erythrocytes
Haemoglobin
Thrombocytes
Haematocrit
Height
Insulin
MCV
Cholesterol
ApoA1

PC3

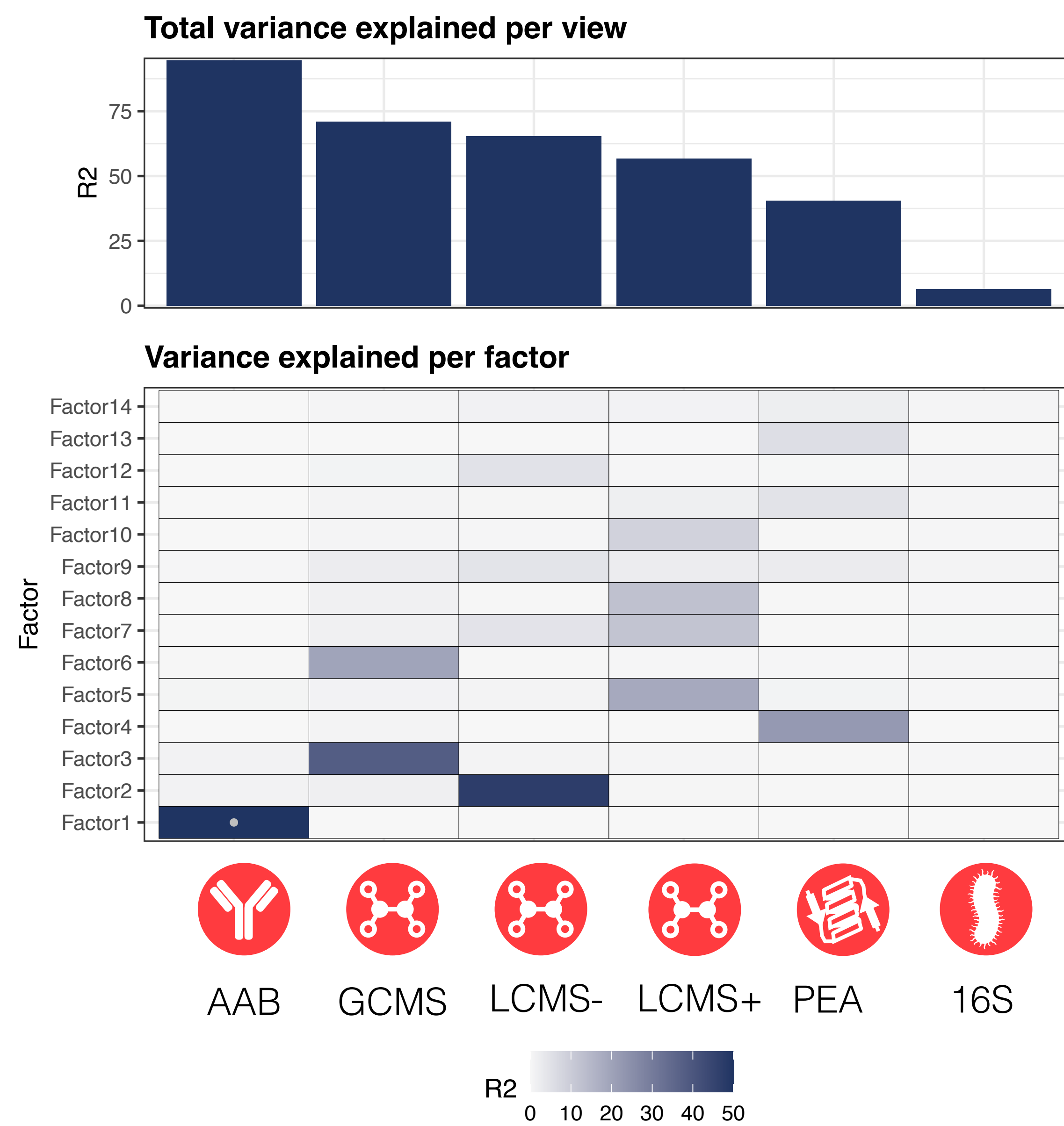


Cholesterol
LDL cholesterol
ApoB
Age
ApoA1
Insulin

bioRxiv preprint doi: <https://doi.org/10.1101/2020.11.11.365387>; this version posted November 12, 2020. The copyright holder for this preprint (which was not certified by peer review) is the author/funder, who has granted bioRxiv a license to display the preprint in perpetuity. It is made available under aCC-BY-NC-ND 4.0 International license.

Figure 2: A. Longitudinal analysis reveals the positive effect of data feedback and coaching on health. Generalized Estimating Equation (GEE) model prediction for the significantly changed variables (FDR<0.05), stratified by sex and out/within range status at baseline. For this analysis, the second visit represented a baseline because data feedback and coaching started at the 2nd and 3rd visits respectively (blue: within range, red: out of range). Bootstrapped confidence intervals are shown. **B.** Principal components plot of the individuals obtained using all the numerical clinical variables. The trajectories for two selected individuals along successive study visits are shown with arrows. The loadings for the first three PCs are shown in the bottom panels and the variables with relative contribution higher than average (red line) are named.

A



B

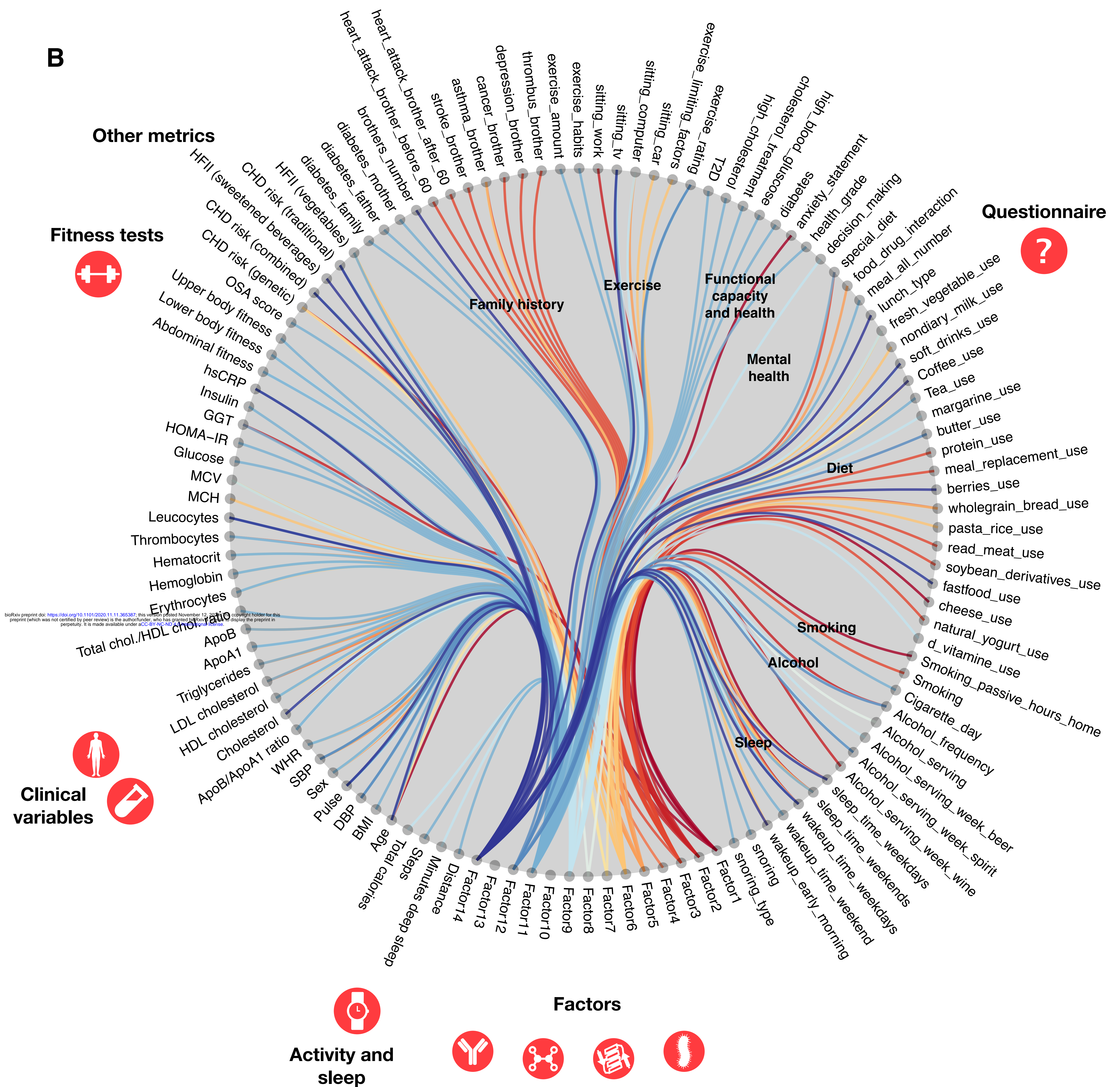
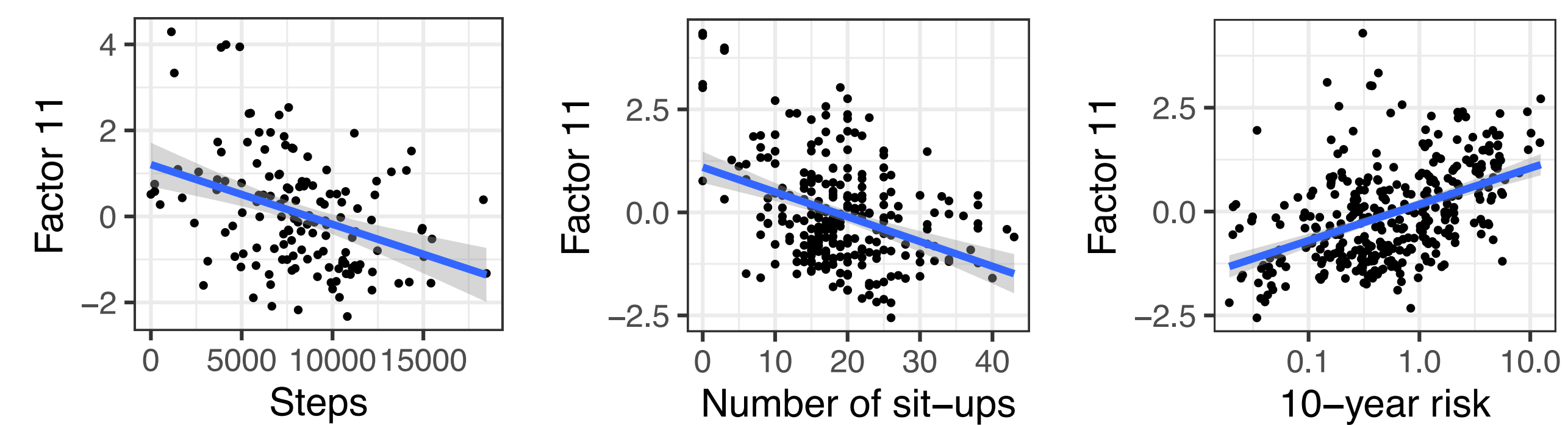
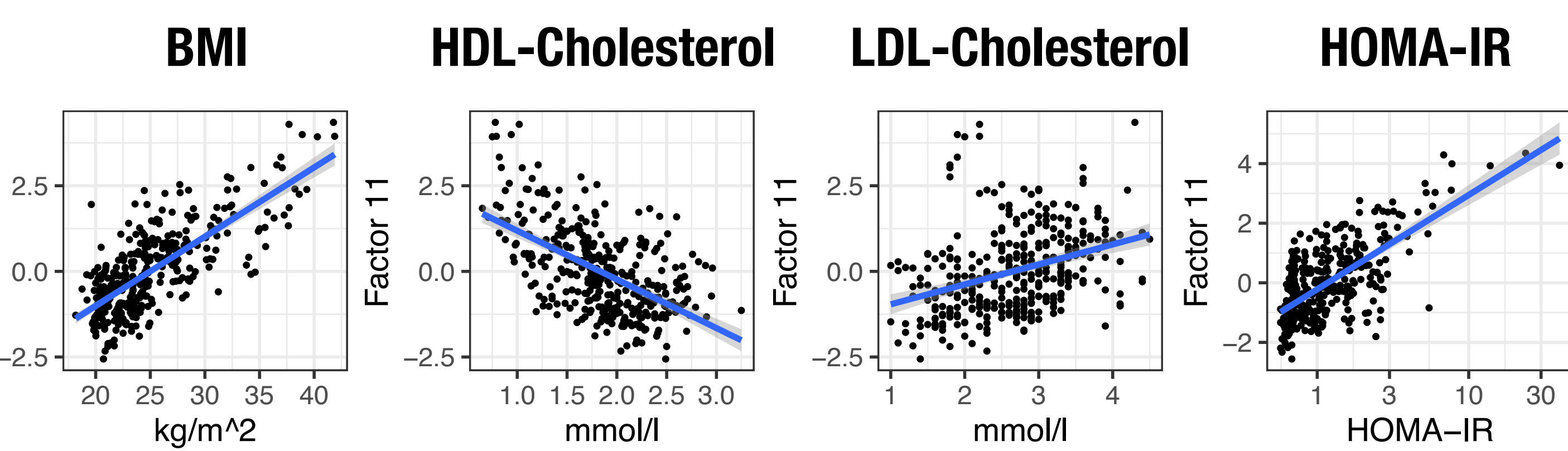
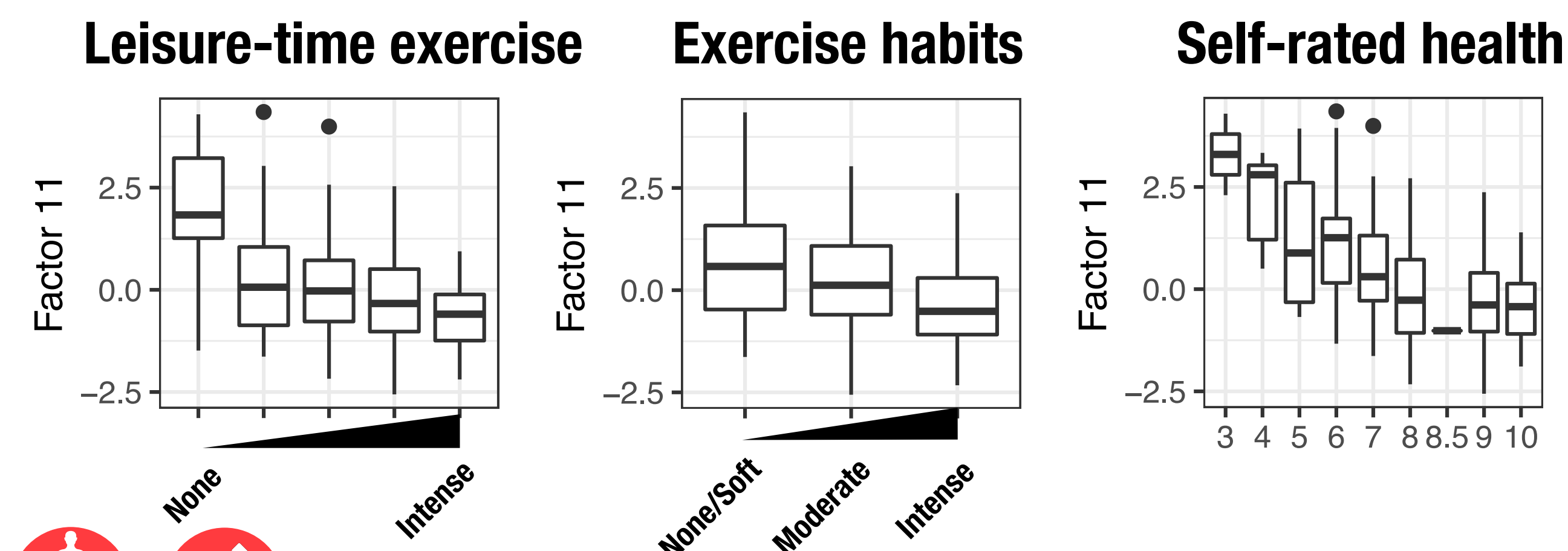
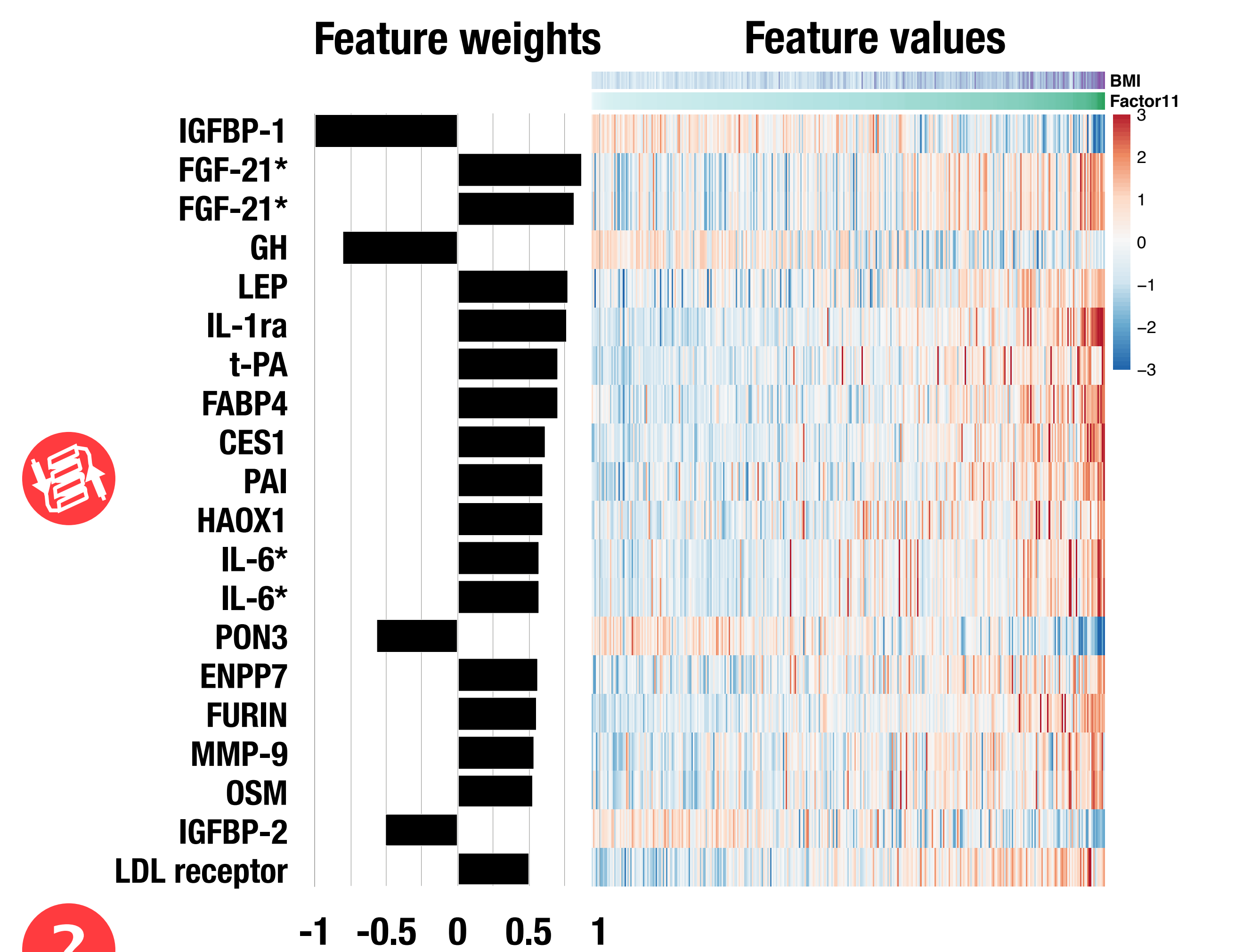
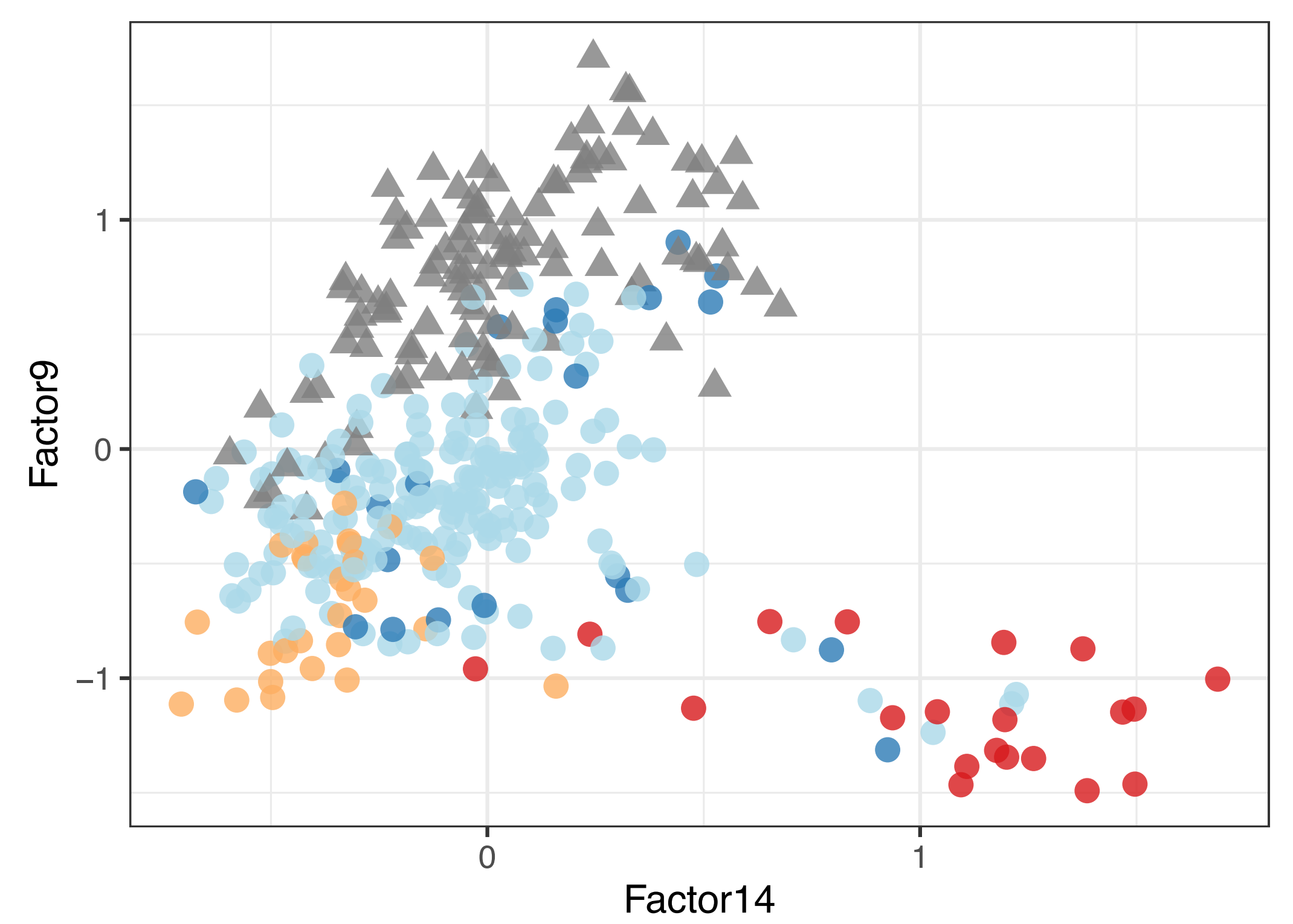


Figure 3. A. Variance decomposition. Percentage of total variance explained (R^2) for each data layer (up) or variance explained (R^2) for each factor and data layer (bottom). A dot marks the out-of-bound value ($>50\%$) for autoantibodies. **B.** Association with phenotype. The factor values were tested for their association with the phenotypic variables and the top associations ($FDR < 0.001$) are shown. The edges are bundled according to their category and colored based on the originating factor.

A Factor 11: obesity and insulin resistance

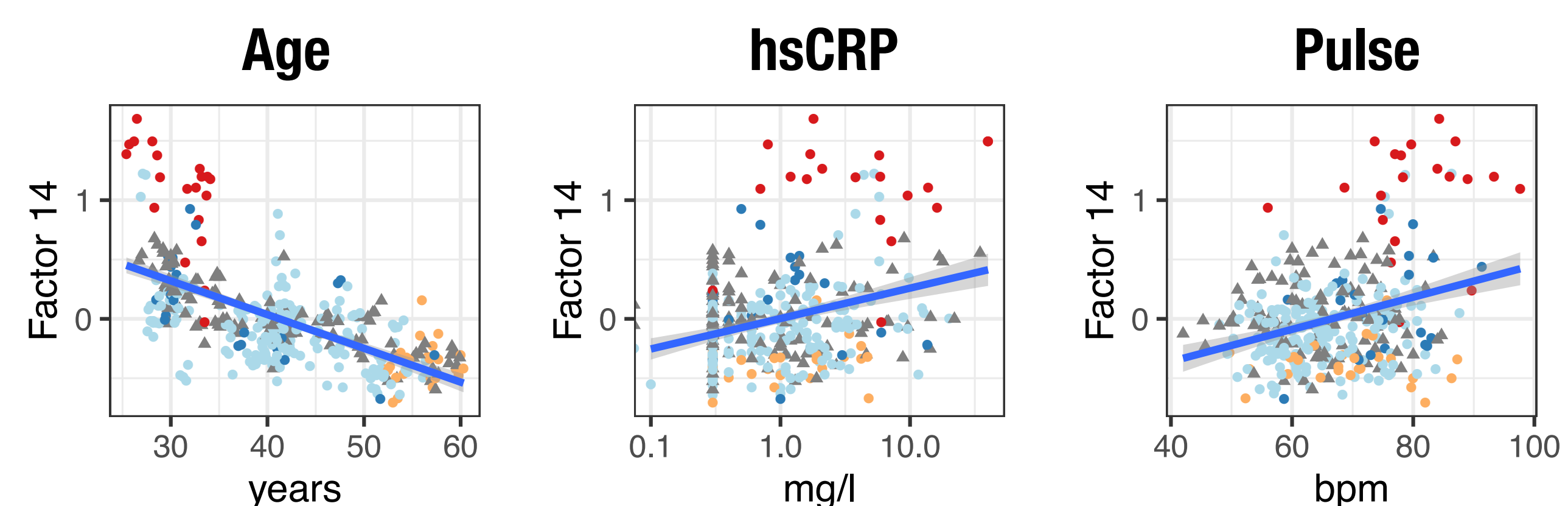
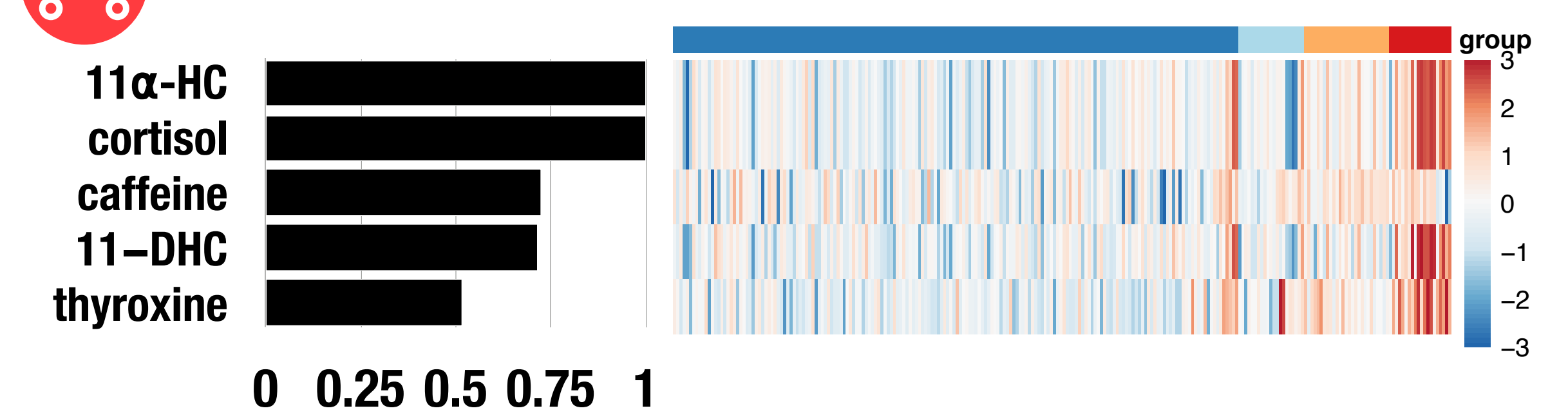
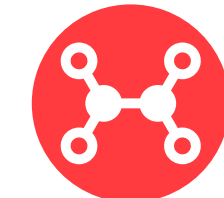
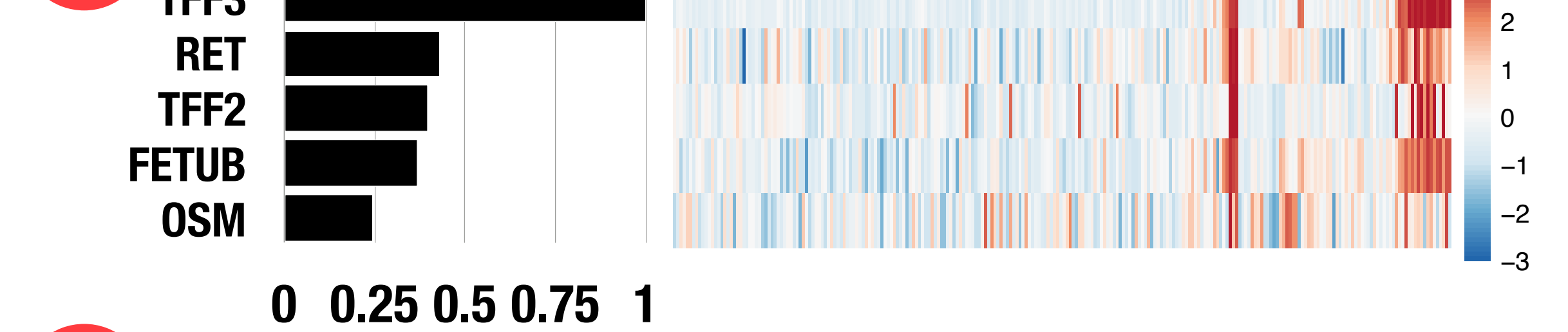


B Factor 14: Hormonal influences



● contraceptive with ethinyl estradiol ● no hormones
● menopausal hormone therapy ● other contraceptive

● F ▲ M



bioRxiv preprint doi: <https://doi.org/10.1101/2020.11.11.365387>; this version posted November 12, 2020. The copyright holder for this preprint (which was not certified by peer review) is the author/funder, who has granted bioRxiv a license to display the preprint in perpetuity. It is made available under aCC-BY-NC-ND 4.0 International license.

C

Factor 7: Diet (coffee)

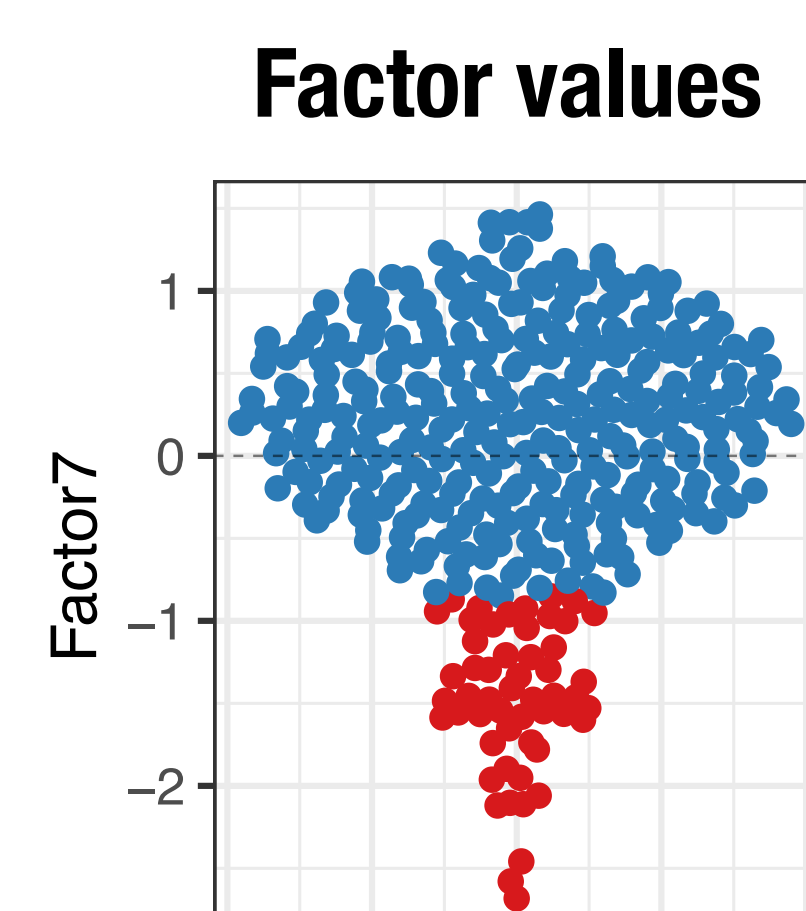
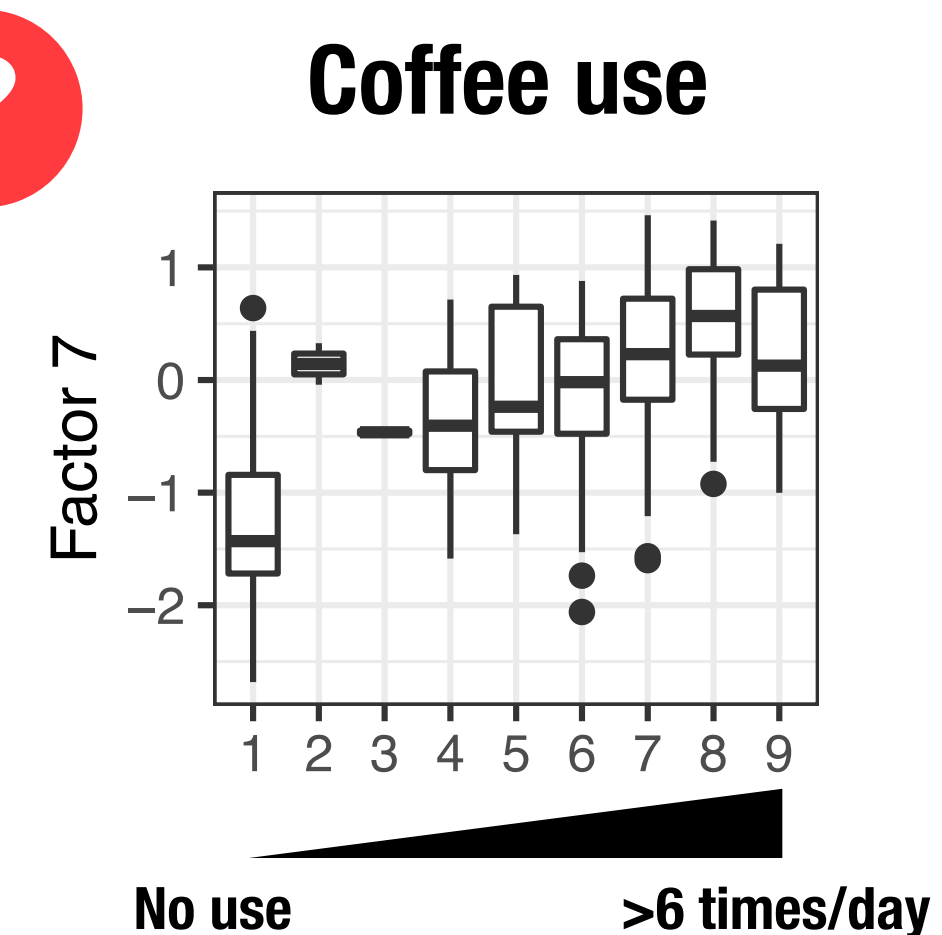
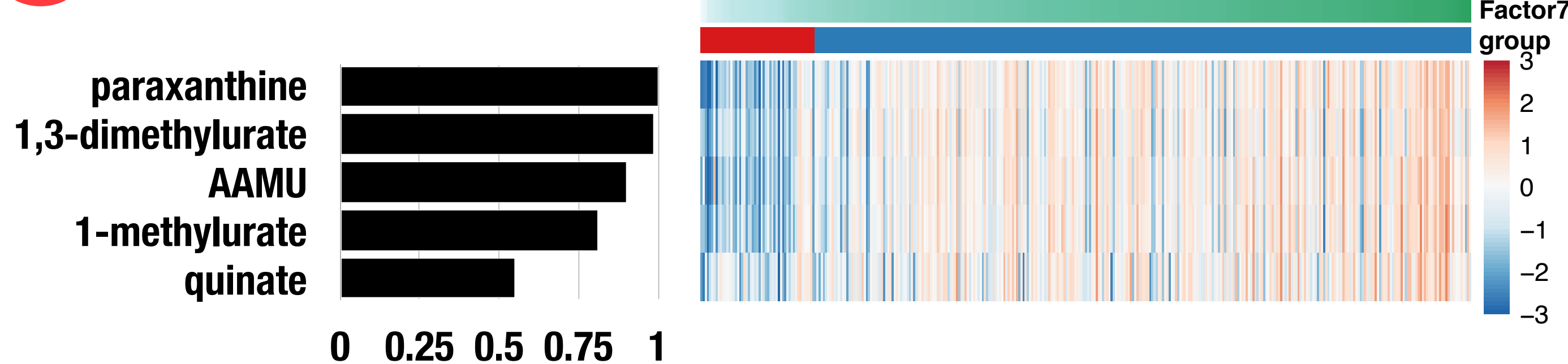
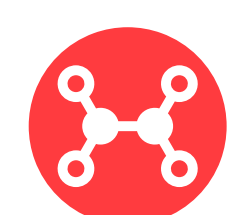
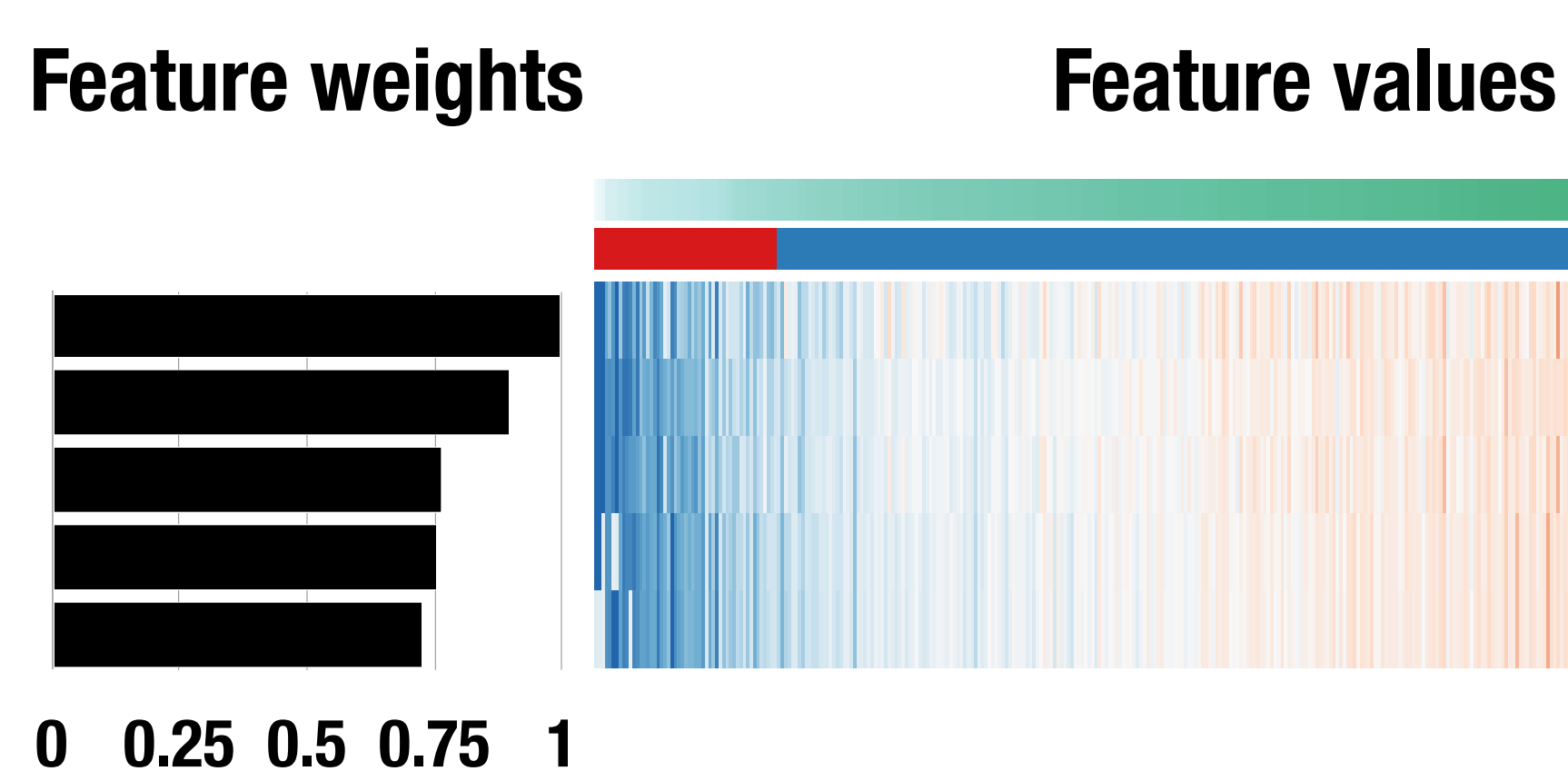
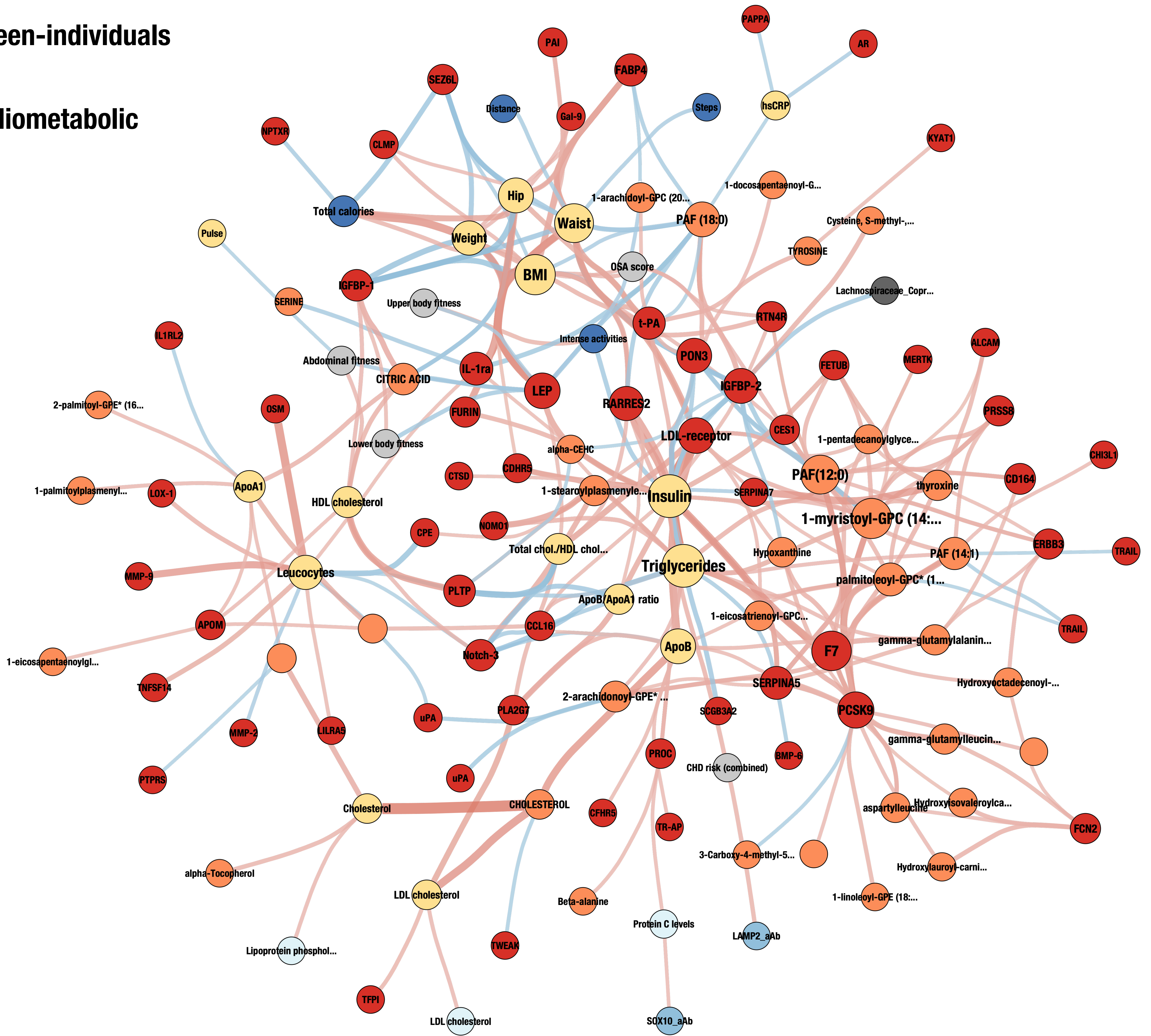


Figure 4. A. Factor11 is linked to obesity and insulin sensitivity. The top scaled protein weights for Factor11 are shown as well as their values (row z-score). The association between the factor values for each sample and the phenotypic variables is shown. A regression line with 95% confidence interval is shown when appropriate. An asterisk marks the proteins measured on multiple PEA panels. **B.** Factor14 is influenced by hormones. A scatterplot of Factor9 and Factor14 values shows that samples can be separated based on the sex (Factor9) and the use of hormones (Factor14). Factor14 identifies a group of young women using contraceptives with ethinyl estradiol (red). The top metabolites and proteins with positive scaled weights on Factor14 are shown. The original feature values are shown as a heatmap (row z-score). The association between the factor values for each sample and the phenotypic variables is shown, as well as a regression line with 95% confidence interval. Points are coloured as in the top panel. Abbreviations: 11 α -HC: 11alpha-hydrocortisone, 11-DHC: 11-dehydrocorticosterone. **C.** Factor7 is associated to coffee consumption. The scaled positive weights are shown for the top metabolites, as well as their values. The association between the factor values with self-reported coffee consumption is shown. A two-group classification of the samples based on Factor7 values was obtained with gaussian-mixture modeling and shown with colored dots (red: lower coffee consumption, blue: higher coffee consumption).

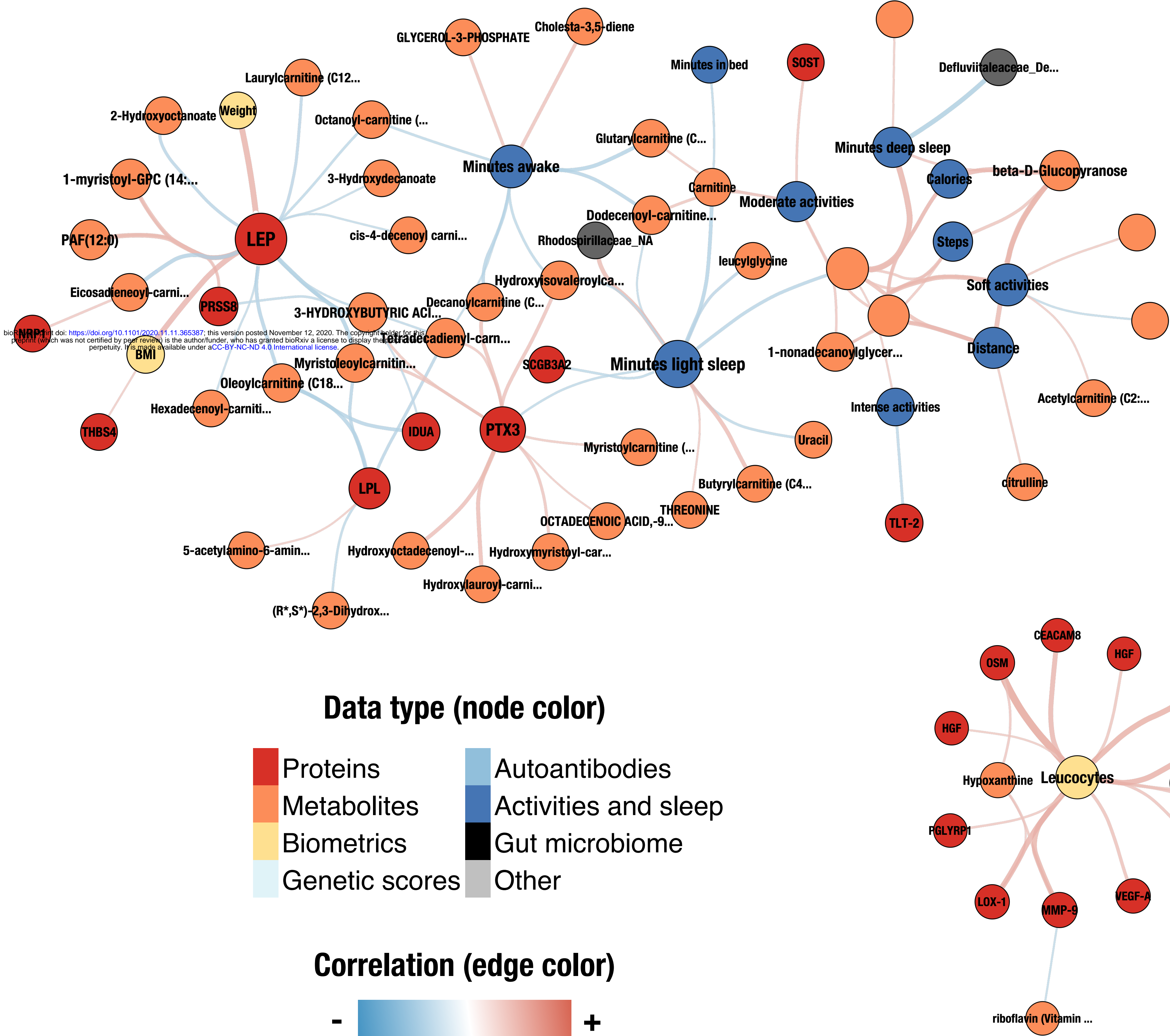
A Between-individuals

Cardiometabolic

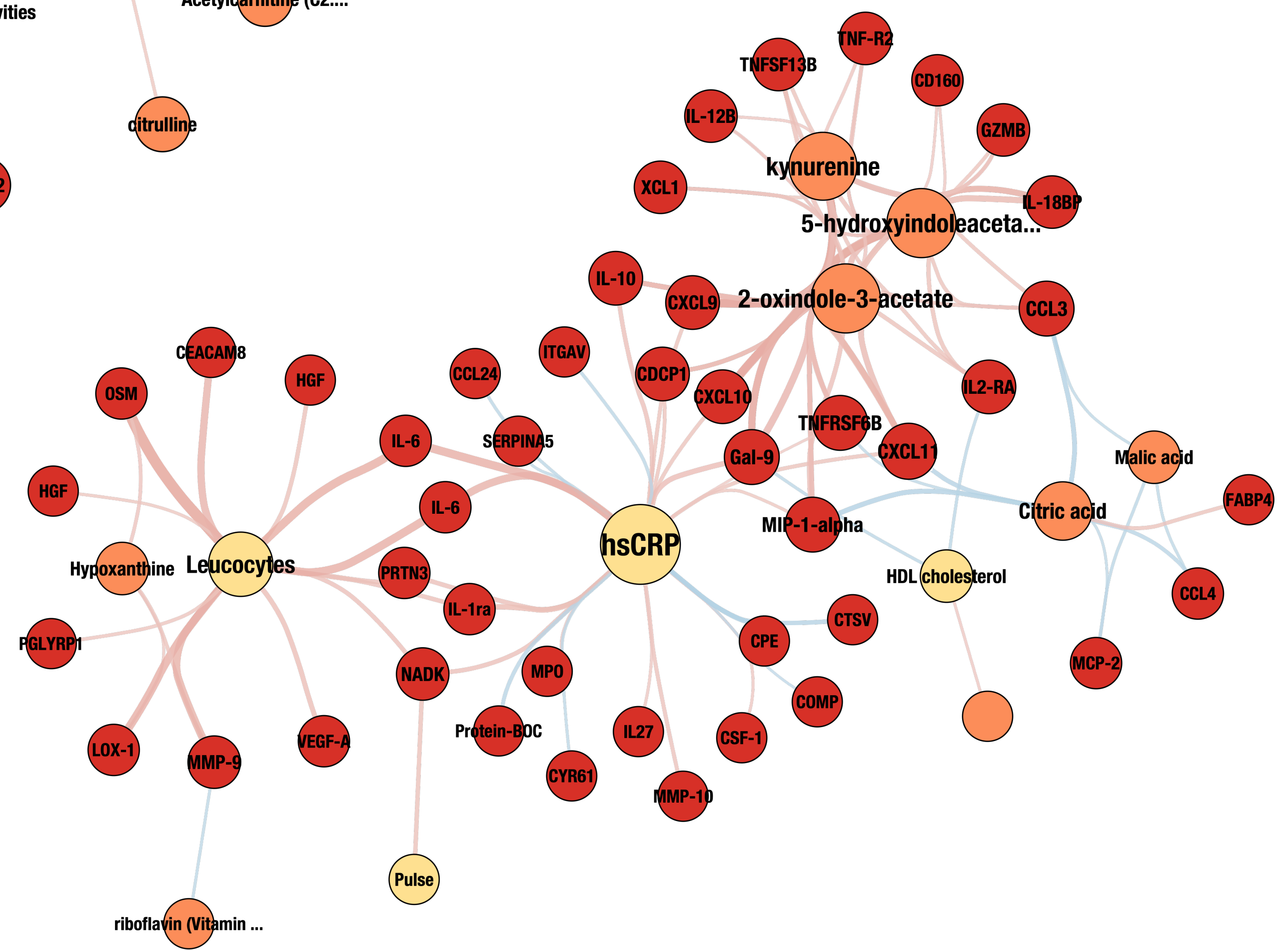


B Within-individuals

Activity and sleep



Inflammation



Data type (node color)

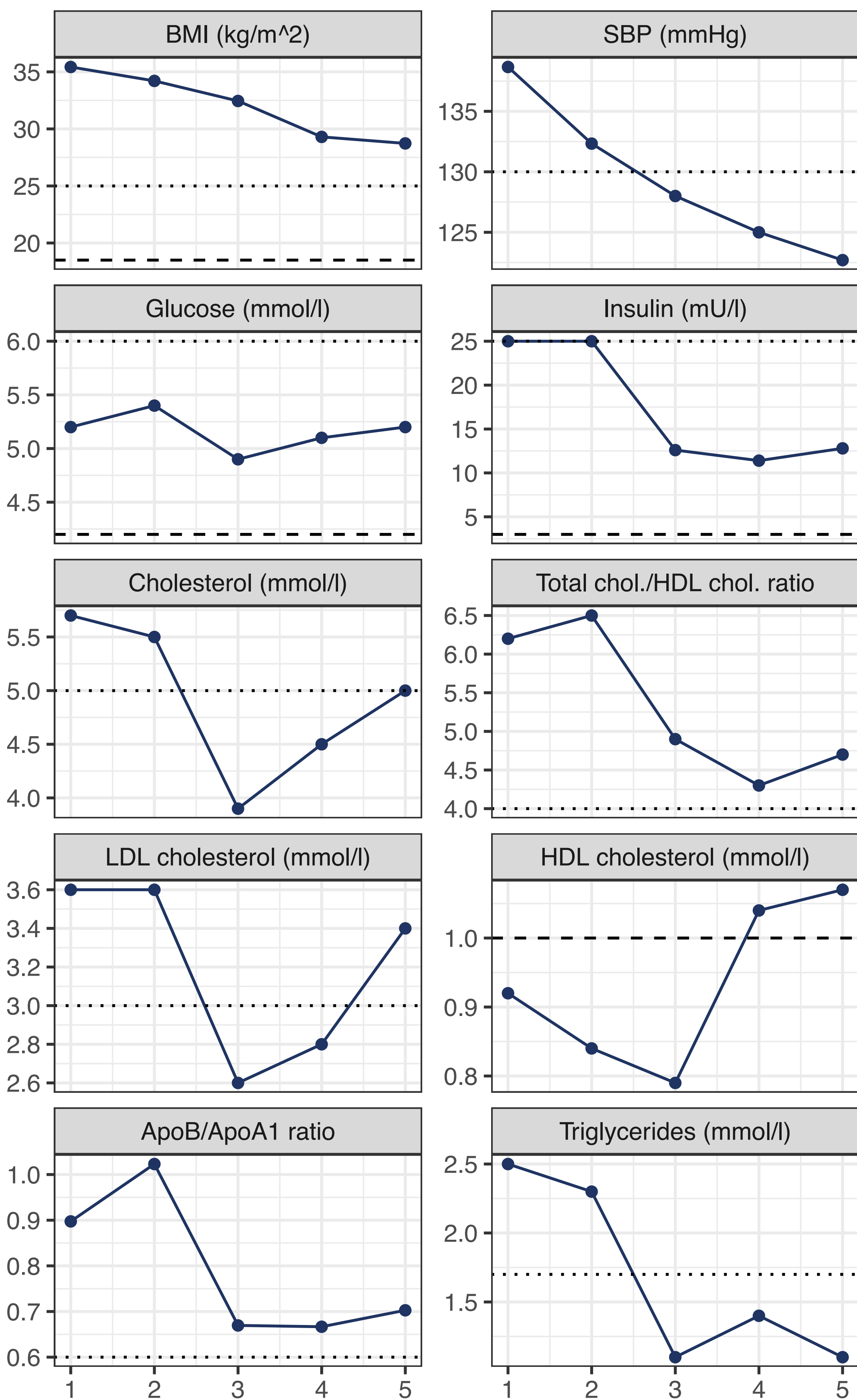
- Proteins
- Metabolites
- Biometrics
- Genetic scores
- Autoantibodies
- Activities and sleep
- Gut microbiome
- Other

Correlation (edge color)

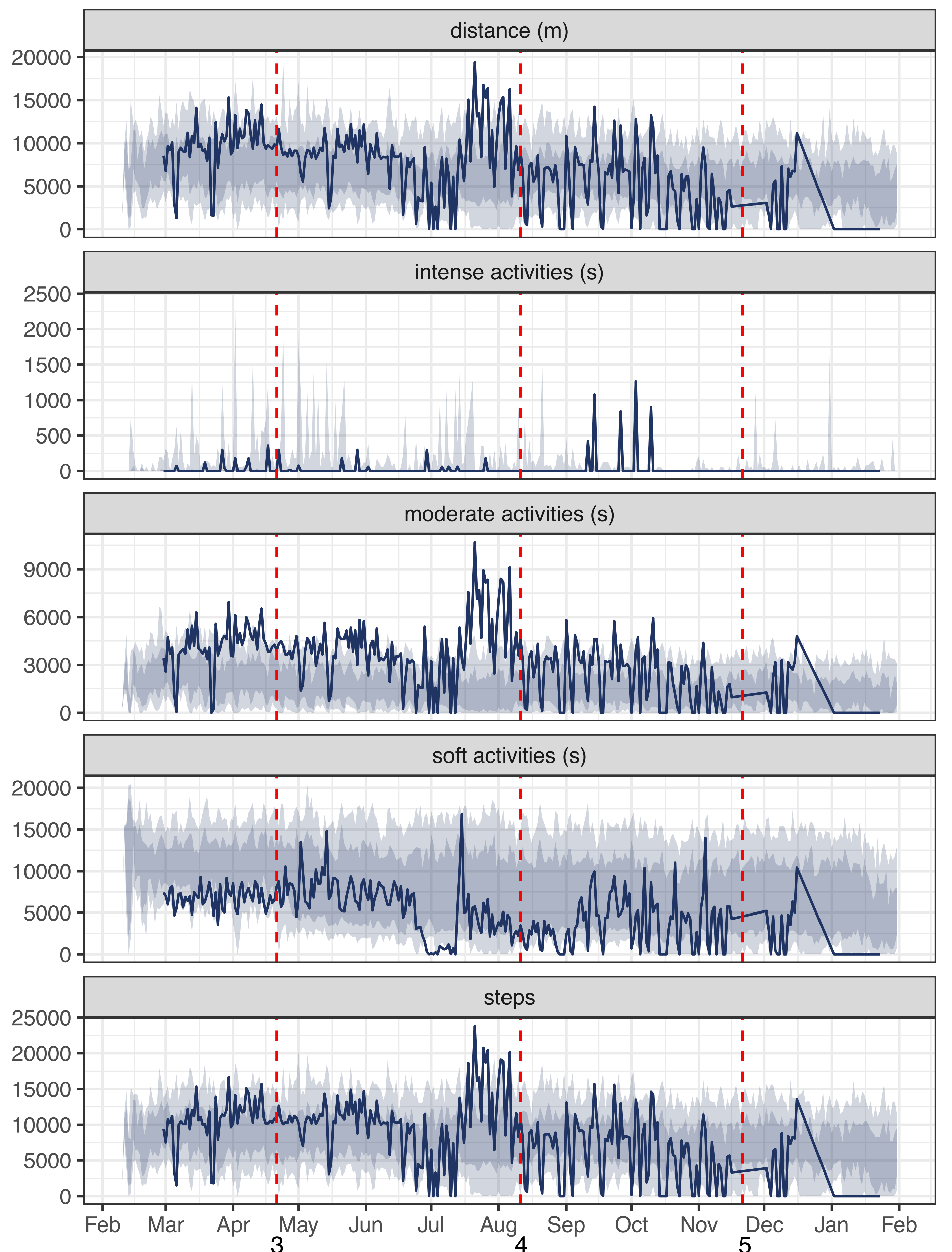


Figure 5. Cross-correlation network analysis aids the interpretation the relationship between data types. Only associations between features of different type were considered to calculate correlation networks at $FDR < 0.05$. The size of the nodes is proportional to the node degree and the edge thickness is proportional to the magnitude of the correlation. The node color indicate different data types. The proteins appearing twice in the network were measured on multiple PEA panels. **A.** Selected between-individual subnetwork. **B.** Selected within-individual network modules.

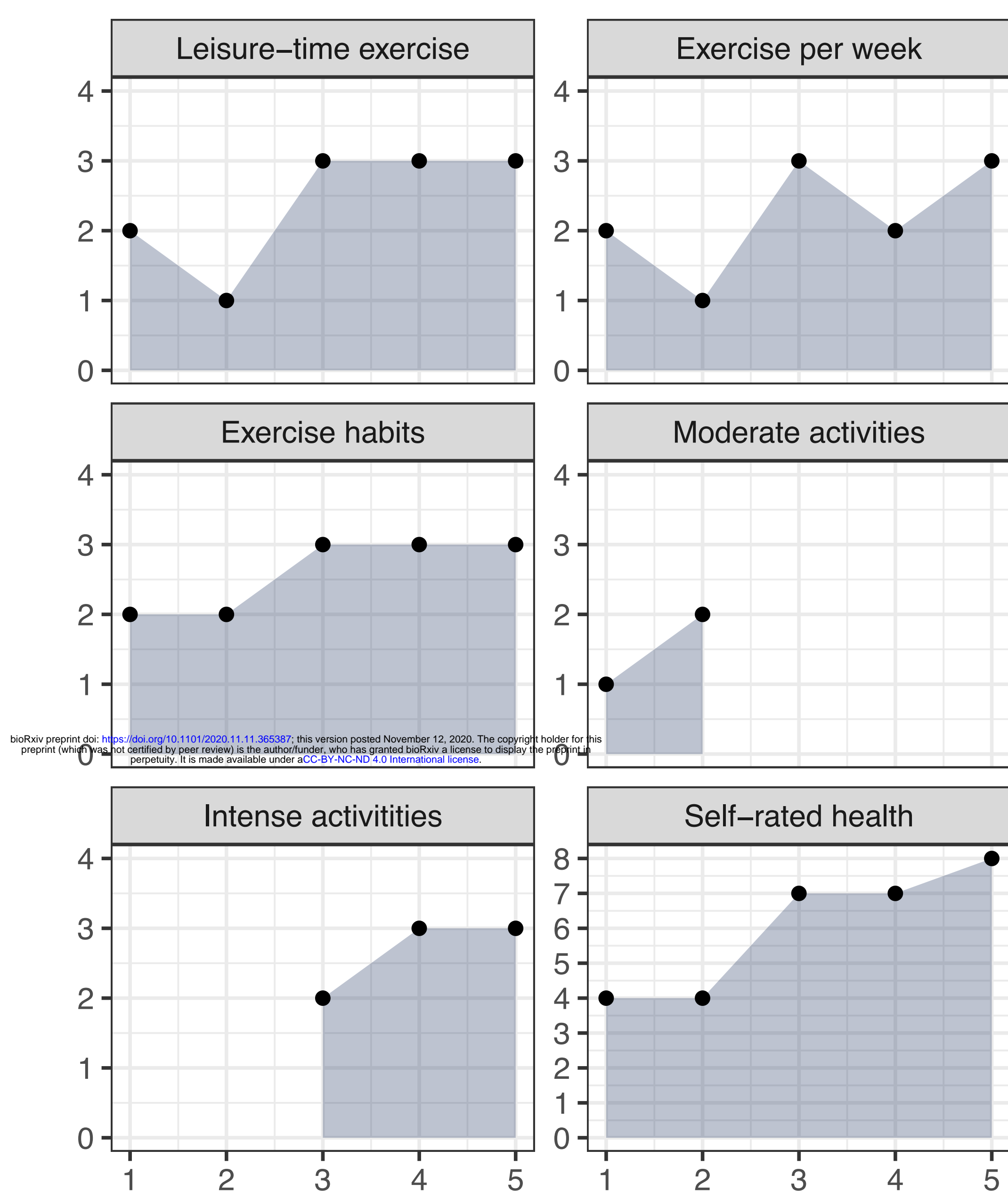
A Clinical variables



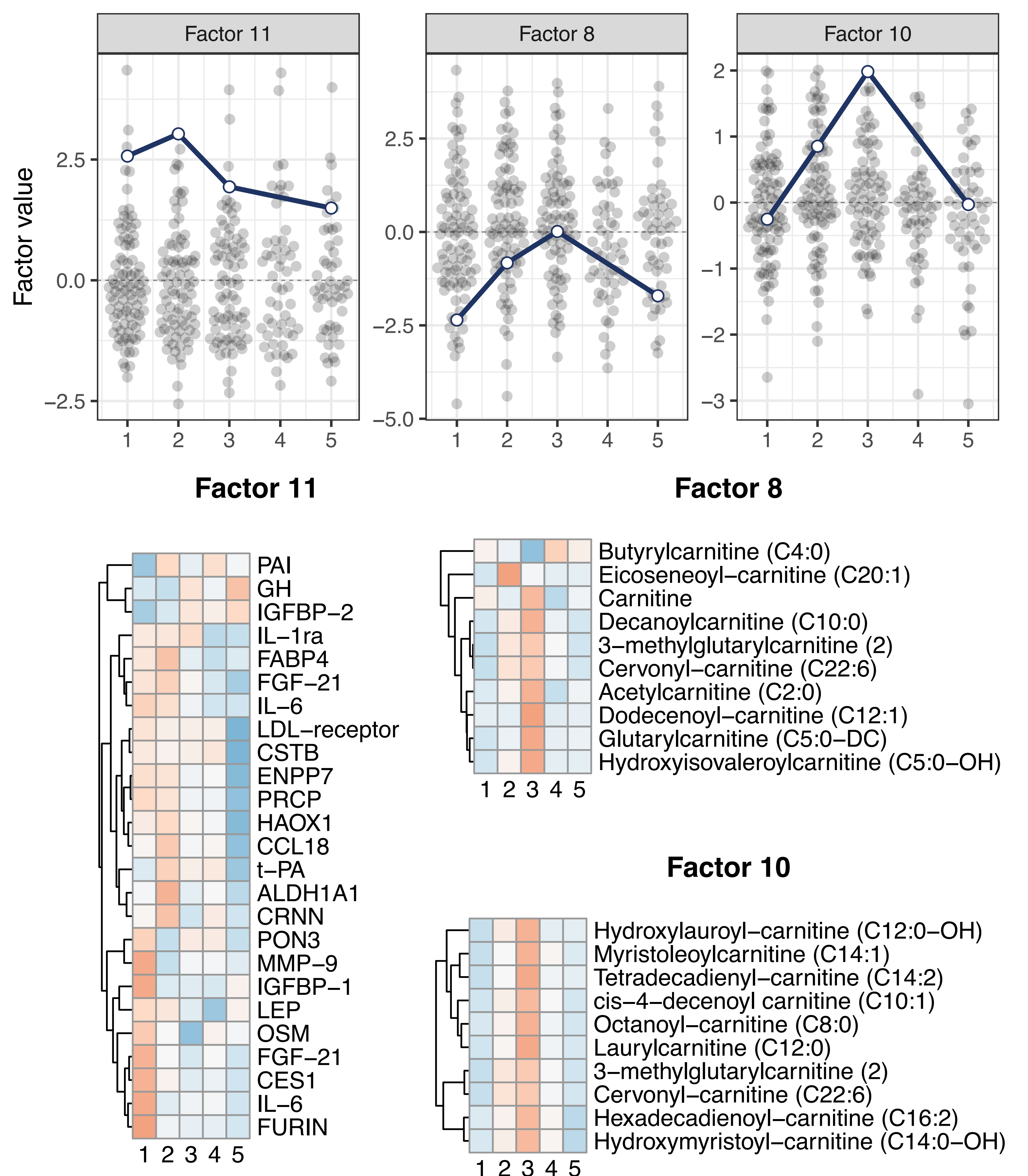
B Activities



C Questionnaire



D MOFA



E Gut microbiome diversity

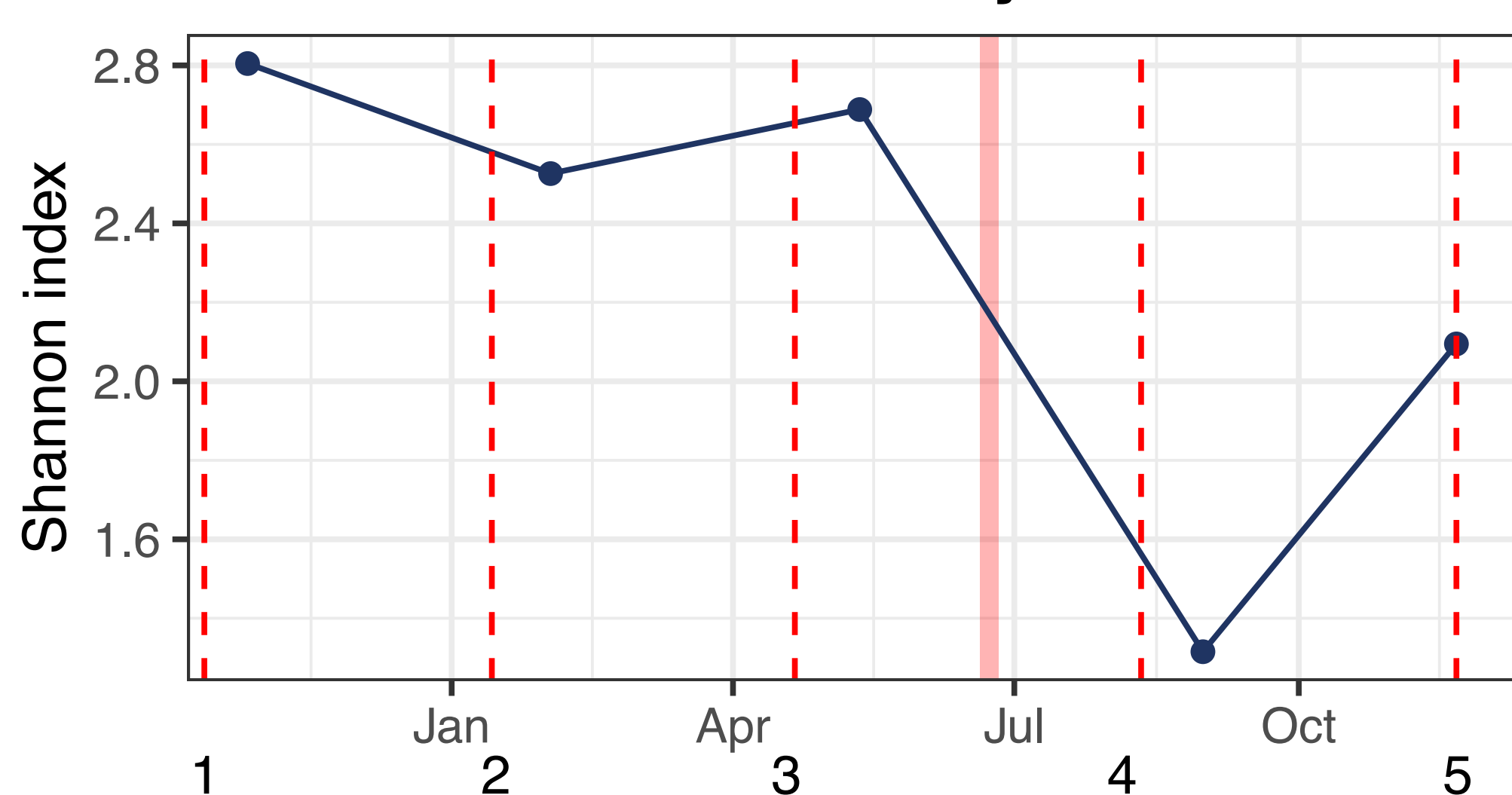


Figure 6. A case study: lifestyle change in one individual and the associated molecular changes. **A.** Clinical variables showing longitudinal changes. Reference values are shown (dashed line: lower normal value, dotted line: upper normal value) **B.** Daily summary of the activities recorder by the smart watch included: distance, time spent in intense, moderate or soft activities and number of steps. The shaded area correspond to the 10, 25, 75 and 90 percentiles in the whole population. The study visits are marked with vertical dashed lines **C.** Selected lifestyle questions. The numbers correspond to orderer categories, where a higher number corresponds to higher frequency or more favorable outcome. **D.** Longitudinal values for selected MOFA+ factors (blue line) plotted together with the factor values for the remaining samples at each study visit (grey dots). **E.** Gut microbiome diversity (Shannon index). The vertical dashed line mark the date for the study visit, which could be different than the fecal sample collection date (dots). A red shaded area mark a period of antibiotic treatment.

774

Supplementary Table 1

	Unit	Value at baseline (n=96)
Age	years (mean ± SE)	40.9 ± 0.9
Sex	counts (M/F)	30/66
BMI	kg/m ² (mean ± SE)	24.9 ± 0.5
Alcohol consumption	g/week (mean ± SE)	53.1 ± 5.4
Current smokers¹	%	16 ²
Education >12 years	%	87
Physical exercise ≥ 3 times/week	%	56
Married or cohabiting	%	67
Hypercholesterolemia (Cholesterol > 5 mmol/l)	%	44
Hypertriglyceridemia (Females: 20-30y, >1.5; 30-50y, >1.7; >50y, >2 Males: 20-30y, >1.7; >30y, >2)	%	4
Overweight or obesity (BMI > 25 kg/m ²)	%	38
Elevated blood pressure (SBP > 130 mmHg)	%	31
Low vitamin D (25(OH)D < 50 nmol/l)	%	31
Hyperglycemia (Fasting glucose > 6 nmol/l)	%	8
Anemia (Hb < 117 (F) or Hb < 134 (M) g/l)	%	2
Self-reported obstructive sleep apnea	%	2

776

778

¹ Participants who reported regular smoking were defined as current smokers.

² n=94

Supplementary table 2. List of all the included features and their annotation.

780 (see separate Excel file)

782 **Supplementary table 3. Results from the GEE model**

	Estimate	Units	CI	P-value	FDR	Type	# of OORB
Hip circumference	-0.667	cm	-0.957 – -0.377	6.34E-06	8.87E-05	All	1
25(OH)D	4.072	nmol/l	2.336 – 5.808	4.29E-06	8.87E-05	OORB	24
Systolic blood pressure	-3.078	mmHg	-4.469 – -1.688	1.43E-05	1.33E-04	OORB	27
Diastolic blood pressure	-0.947	mmHg	-1.443 – -0.451	1.81E-04	1.01E-03	OORB	22
Pulse	-3.214	bpm	-4.876 – -1.551	1.52E-04	1.01E-03	OORB	9
Total/HDL cholesterol ratio	-0.405		-0.66 – -0.150	1.88E-03	8.77E-03	OORB	7
LDL cholesterol	-0.085	mmol/l	-0.139 – -0.030	2.21E-03	8.83E-03	OORB	29
ApoB/ApoA1 ratio	-0.014		-0.024 – -0.005	3.89E-03	1.36E-02	OORB	35
Cholesterol	-0.084	mmol/l	-0.145 – -0.024	5.83E-03	1.81E-02	OORB	36

784 **Supplementary table 4. Associations between MOFA factor values and phenotypic**
variables.

786 (see separate Excel file)

788 **Supplementary table 5. Edge lists for the Between- and Within-Individual Networks.**

(see separate Excel file)

790

REFERENCES

- 792 1. Chen, R. *et al.* Personal omics profiling reveals dynamic molecular and medical
phenotypes. *Cell* **148**, 1293–1307 (2012).
- 794 2. Chen, R. *et al.* Longitudinal personal DNA methylome dynamics in a human with a
chronic condition. *Nat Med* **6**, 1 (2018).
- 796 3. Perkins, B. A. *et al.* Precision medicine screening using whole-genome sequencing and
advanced imaging to identify disease risk in adults. *Proc Natl Acad Sci USA* **115**, 3686–
798 3691 (2018).
- 800 4. Piening, B. D. *et al.* Integrative Personal Omics Profiles during Periods of Weight Gain
and Loss. *Cell Systems* **6**, 157–170.e8 (2018).
- 802 5. Price, N. D. *et al.* A wellness study of 108 individuals using personal, dense, dynamic
data clouds. *Nat Biotechnol* **35**, 747–756 (2017).
- 804 6. Zhou, W. *et al.* Longitudinal multi-omics of host-microbe dynamics in prediabetes.
Nature **569**, 663–671 (2019).
- 806 7. Schüssler-Fiorenza Rose, S. M. *et al.* A longitudinal big data approach for precision
health. *Nat Med* **25**, 792–804 (2019).
- 808 8. Ahadi, S. *et al.* Personal aging markers and ageotypes revealed by deep longitudinal
profiling. *Nat Med* **26**, 83–90 (2020).
- 810 9. Tebani, A. *et al.* Integration of molecular profiles in a longitudinal wellness profiling
cohort. *Nat Commun* **11**, 1–14 (2020).
- 812 10. Digital Health Revolution. *digitalhealthrevolution.fi* Available at:
[http://www.digitalhealthrevolution.fi/uploads/2/4/1/5/24155377/person_centric_data_m
anagement_models_and_opportunities_in_health_care_sector_full.pdf](http://www.digitalhealthrevolution.fi/uploads/2/4/1/5/24155377/person_centric_data_management_models_and_opportunities_in_health_care_sector_full.pdf). (Accessed:
814 22nd October 2020)
- 816 11. Argelaguet, R. *et al.* Multi-Omics Factor Analysis—a framework for unsupervised
integration of multi-omics data sets. *Mol Syst Biol* **14**, e8124 (2018).
- 818 12. Argelaguet, R. *et al.* MOFA+: a probabilistic framework for comprehensive integration
of structured single-cell data. *bioRxiv* **18**, 837104 (2019).
- 820 13. Considine, R. V. *et al.* Serum immunoreactive-leptin concentrations in normal-weight
and obese humans. *N Engl J Med* **334**, 292–295 (1996).
- 822 14. Juge-Aubry, C. E. *et al.* Adipose tissue is a major source of interleukin-1 receptor
antagonist: upregulation in obesity and inflammation. *Diabetes* **52**, 1104–1110 (2003).
- 824 15. Zheng, Z. *et al.* Interacting hepatic PAI-1/tPA gene regulatory pathways influence
impaired fibrinolysis severity in obesity. *J. Clin. Invest.* **130**, 4348–4359 (2020).
- 826 16. Xu, A. *et al.* Adipocyte fatty acid-binding protein is a plasma biomarker closely
associated with obesity and metabolic syndrome. *Clinical Chemistry* **52**, 405–413
(2006).
- 828 17. Fisher, F. M. *et al.* Obesity is a fibroblast growth factor 21 (FGF21)-resistant state.
Diabetes **59**, 2781–2789 (2010).
- 830 18. Mayne, J. *et al.* Associations Between Soluble LDLR and Lipoproteins in a White
Cohort and the Effect of PCSK9 Loss-of-Function. *J. Clin. Endocrinol. Metab.* **103**,
832 3486–3495 (2018).
- 834 19. Kopchick, J. J., Berryman, D. E., Puri, V., Lee, K. Y. & Jorgensen, J. O. L. The effects of
growth hormone on adipose tissue: old observations, new mechanisms. *Nat Rev
Endocrinol* (2019). doi:10.1038/s41574-019-0280-9
- 836 20. Shih, D. M. *et al.* PON3 knockout mice are susceptible to obesity, gallstone formation,
and atherosclerosis. *FASEB J.* **29**, 1185–1197 (2015).
- 838 21. Nam, S. Y. *et al.* Effect of obesity on total and free insulin-like growth factor (IGF)-1,
and their relationship to IGF-binding protein (BP)-1, IGFBP-2, IGFBP-3, insulin, and
840 growth hormone. *Int J Obes* **21**, 355–359 (1997).
- 842 22. Meulenberg, P. M. M., Ross, H. A., Swinkels, L. M. J. W. & Benraad, T. J. The effect of
oral contraceptives on plasma-free and salivary cortisol and cortisone. *Clinica Chimica
Acta* **165**, 379–385 (1987).

- 844 23. Barsivala, V., Virkar, K. & Kulkarni, R. D. Thyroid functions of women taking oral
contraceptives. *Contraception* **9**, 305–314 (1974).
- 846 24. Hodson, L., Skeaff, C. M. & Fielding, B. A. Fatty acid composition of adipose tissue and
848 blood in humans and its use as a biomarker of dietary intake. *Progress in Lipid
Research* **47**, 348–380 (2008).
- 850 25. Ussher, J. R., Elmariah, S., Gerszten, R. E. & Dyck, J. R. B. The Emerging Role of
Metabolomics in the Diagnosis and Prognosis of Cardiovascular Disease. *J. Am. Coll.
Cardiol.* **68**, 2850–2870 (2016).
- 852 26. Egan, B. M., Greene, E. L. & Goodfriend, T. L. Nonesterified fatty acids in blood
854 pressure control and cardiovascular complications. *Curr. Hypertens. Rep.* **3**, 107–116
(2001).
- 856 27. Neiman, M. *et al.* Individual and stable autoantibody repertoires in healthy individuals.
Autoimmunity **52**, 1–11 (2019).
- 858 28. Rubtsova, K., Rubtsov, A. V., Cancro, M. P. & Marrack, P. Age-Associated B Cells: A T-
bet-Dependent Effector with Roles in Protective and Pathogenic Immunity. *J Immunol*
195, 1933–1937 (2015).
- 860 29. Prentice, K. J. *et al.* CMPF, a Metabolite Formed Upon Prescription Omega-3-Acid
862 Ethyl Ester Supplementation, Prevents and Reverses Steatosis. *EBioMedicine* **27**, 200–
213 (2018).
- 864 30. Paige, E. *et al.* Interleukin-6 Receptor Signaling and Abdominal Aortic Aneurysm
Growth Rates. *Circ Genom Precis Med* **12**, e002413 (2019).
- 866 31. Ristagno, G. *et al.* Pentraxin 3 in Cardiovascular Disease. *Front Immunol* **10**, 1357
(2019).
- 868 32. Bonacina, F. *et al.* Pentraxin 3 deficiency protects from the metabolic inflammation
associated to diet-induced obesity. *Cardiovasc Res* **115**, 1861–1872 (2019).
- 870 33. Wilson, A. M. *et al.* Neuropilin-1 expression in adipose tissue macrophages protects
against obesity and metabolic syndrome. *Sci Immunol* **3**, (2018).
- 872 34. Frateschi, S. *et al.* PAR2 absence completely rescues inflammation and ichthyosis
caused by altered CAP1/Prss8 expression in mouse skin. *Nat Commun* **2**, 161 (2011).
- 874 35. Pan, W. & Kastin, A. J. Leptin: a biomarker for sleep disorders? *Sleep Med Rev* **18**,
283–290 (2014).
- 876 36. Ishibashi, Y. *et al.* Serum TFF1 and TFF3 but not TFF2 are higher in women with breast
cancer than in women without breast cancer. *Sci. Rep.* **7**, 4846 (2017).
- 878 37. Floehr, J. *et al.* Association of high fetuin-B concentrations in serum with fertilization
rate in IVF: a cross-sectional pilot study. *Hum. Reprod.* **31**, 630–637 (2016).
- 880 38. Meex, R. C. *et al.* Fetuin B Is a Secreted Hepatocyte Factor Linking Steatosis to
Impaired Glucose Metabolism. *Cell Metab* **22**, 1078–1089 (2015).
- 882 39. Zubair, N. *et al.* Genetic Predisposition Impacts Clinical Changes in a Lifestyle
Coaching Program. *Sci. Rep.* **9**, 6805 (2019).
- 884 40. Walker, C. G. *et al.* Genetic predisposition to an adverse lipid profile limits the
improvement in total cholesterol in response to weight loss. *Obesity (Silver Spring)* **21**,
2589–2595 (2013).
- 886 41. Okada, Y. & Kamatani, Y. Common genetic factors for hematological traits in humans.
J. Hum. Genet. **57**, 161–169 (2012).
- 888 42. Dopico, X. C. *et al.* Widespread seasonal gene expression reveals annual differences in
human immunity and physiology. *Nat Commun* **6**, 7000 (2015).
- 890 43. Lakshmikanth, T. *et al.* Human immune system variation during one year. *biorxiv* **17**,
2020.01.22.915025 (2020).
- 892 44. Widén, E. & Ripatti, S. Assessment of multifactorial coronary artery disease by utilizing
genomic data. *Duodecim* **133**, 776–781 (2017).
- 894 45. Niiranen, T. J., Kronholm, E., Rissanen, H., Partinen, M. & Jula, A. M. Self-reported
896 obstructive sleep apnea, simple snoring, and various markers of sleep-disordered
breathing as predictors of cardiovascular risk. *Sleep Breath* **20**, 589–596 (2016).
- 898 46. Meinilä, J. *et al.* Healthy Food Intake Index (HFII) - Validity and reproducibility in a
gestational-diabetes-risk population. - PubMed - NCBI. *BMC Public Health* **16**, 3
(2016).

- 900 47. Honko, H. *et al.* W2E--Wellness Warehouse Engine for Semantic Interoperability of
Consumer Health Data. *IEEE J Biomed Health Inform* **20**, 1632–1639 (2016).
- 902 48. Dressendörfer, R. A., Kirschbaum, C., Rohde, W., Stahl, F. & Strasburger, C. J.
Synthesis of a cortisol-biotin conjugate and evaluation as a tracer in an immunoassay
904 for salivary cortisol measurement. *J. Steroid Biochem. Mol. Biol.* **43**, 683–692 (1992).
- 906 49. Pruessner, J. C., Kirschbaum, C., Meinlschmid, G. 2003. Two formulas for computation
of the area under the curve represent measures of total hormone concentration versus
time-dependent change. *Elsevier* doi:10.1016/S0306-4530(02)00108-7
- 908 50. A, J. *et al.* Extraction and GC/MS analysis of the human blood plasma metabolome.
Anal. Chem. **77**, 8086–8094 (2005).
- 910 51. Schauer, N. *et al.* GC-MS libraries for the rapid identification of metabolites in complex
biological samples. *FEBS Lett* **579**, 1332–1337 (2005).
- 912 52. Diamanti, K. *et al.* Intra- and inter-individual metabolic profiling highlights carnitine and
lysophosphatidylcholine pathways as key molecular defects in type 2 diabetes. *Sci.*
914 *Rep.* **9**, 1–13 (2019).
- 916 53. Hugerth, L. W. *et al.* No distinct microbiome signature of irritable bowel syndrome
found in a Swedish random population. *Gut* **69**, 1076–1084 (2020).
- 918 54. Hugerth, L. W. *et al.* DegePrime, a program for degenerate primer design for broad-
taxonomic-range PCR in microbial ecology studies. *Appl Environ Microbiol* **80**, 5116–
5123 (2014).
- 920 55. Callahan, B. J. *et al.* DADA2: High-resolution sample inference from Illumina amplicon
data. *Nat Meth* **13**, 581–583 (2016).
- 922 56. Gagnon-Bartsch, J. A., Jacob, L., Univ, T. S. T. R. F. D. S. 2013. Removing unwanted
variation from high dimensional data with negative controls.
- 924 57. Dieterle, F., Ross, A., Schlotterbeck, G. & Senn, H. Probabilistic quotient normalization
as robust method to account for dilution of complex biological mixtures. Application in
926 ¹H NMR metabonomics. *Anal. Chem.* **78**, 4281–4290 (2006).
- 928 58. Bakdash, J. Z. & Marusich, L. R. Repeated Measures Correlation. *Front Psychol* **8**, 456
(2017).